Measurement of trace components in aqueous solutions with near and mid infrared Fourier transform spectroscopy

Peter Snoer Jensen

Lund Reports on Atomic Physics
LRAP-299

Doctoral Thesis
Department of Physics
Lund Institute of Technology
March 2003

LUND INSTITUTE OF TECHNOLOGY
Lund University

This thesis was typeset by the author on an Intel based computer running the Gnu/Linux operating system with the command:

```
cat thesis.ms|soelim|refer|tbl|pic|eqn|groff -ms -P-g >thesis.ps
```

and afterwards transformed from postscript format into pdf format with pstopdf.

Vi, ed and ghostview were used for editing and viewing the thesis. Data were processed using ANSI C programs based on routines from Numerical Recipes in C by Press et al. and compiled with the GCC compiler. sh scripts, sed and AWK filters were used to automate complicated calculations. Visualization and graphs were prepared using Gnuplot. The scientific papers were written using the TEX system. The author warmly recommends these tools.

Printed by Pittney Bowes Management Services, DK
March 2003

Lund Reports on Atomic Physics, LRAP-299
ISSN 0281-2162
LUTFD2(TFAF-1052)/1-54(2003)
ISBN 91-628-5587-5

LUND INSTITUTE OF TECHNOLOGY
Lund University

Contents

Abstract

This thesis treats various aspects of the measurement of trace components in aqueous solutions with Fourier transform infrared spectroscopy. This technique has several applications from such diverse fields as dairy industry and biomedical optics. The use of infrared spectroscopy for trace component quantification is made difficult by the large absorption of water which dominates the spectrum. The signals from the trace components are small in comparison and must be detected under circumstances where the water spectrum determines both instrument configuration and usable wavenumber regions. In addition the absorption of water may be changed by the presence of other components in the solution or by variations in temperature. The papers, upon which this thesis is based are concerned with several aspects relating to this problem. The influence of the water absorption spectrum and the configuration of spectrometers are discussed. One publication treats the problem of selection of optimal transmission cell pathlength for measurement of trace components in aqueous solutions. Another publication presents a dual-beam, optical null, Fourier transform spectrometer for measurements of trace components in the near infrared spectral range that offers an improvement compared to traditional Fourier transform spectrometers. A third publication presents measurements of the temperature induced variations of the absorption spectrum of water and of aqueous solutions of glucose. In addition, two specific applications, both concerning the measurement of trace components in spent dialysate, are demonstrated. One manuscript describes the application of the the dual-beam spectrometer to measure real-time, on-line concentrations of urea in spent dialysate during treatment of patients. Finally, a manuscript demonstrates the feasability of simultaneous measurement of urea, phosphate, and glucose concentrations in spent dialysate with mid infrared transmission spectroscopy.

List of Papers

This thesis is based upon the following papers:

I Peter Snoer Jensen and Jimmy Bak, ‘‘Measurements of Urea and Glucose in Aqueous Solutions with Dual-Beam Near-Infrared Fourier-Transform Spectroscopy’’ *Appl. Spectrosc.* **56,** 12, pp. 1593-1599 (2002)

II Peter Snoer Jensen and Jimmy Bak, ‘‘Near-Infrared Transmission Spectroscopy of Aqueous Solutions: The Influence of Optical Pathlength on Signal-To-Noise Ratio’’, *Appl. Spectrosc.* **56,** 12, pp. 1600-1606 (2002)

III Peter Snoer Jensen, Jimmy Bak, and Stefan Andersson-Engels, ‘‘The Influence of Temperature on Water and Aqueous Glucose Absorption Spectra in the Near- and Mid-Infrared Regions at Physiologically Relevant Temperatures’’ *Appl. Spectrosc.* **57,** 1, pp. 28-36 (2003)

IV Peter Snoer Jensen, Jimmy Bak, Søren Ladefoged, and Stefan Andersson-Engels, ‘‘On-line monitoring of urea concentration in dialysate with dual-beam Fourier transform near infrared spectroscopy’’ Manuscrip submitted to J. Biomed. Opt.

V Peter Snoer Jensen, Jimmy Bak, Søren Ladefoged, and Stefan Andersson-Engels ‘‘Determination of urea, glucose, and phosphate in dialysate with Fourier transform infrared spectroscopy’’ Manuscript submitted to Spectrochim. Acta. Part A.

Additional material

Poster presentation at the Photonics West SPIE conference 2002 in San Jose CA: Peter Snoer Jensen, Jimmy Bak, Peter E. Andersen, and Stefan Andersson-Engels ‘‘Fourier Transform Infrared Spectroscopy of Aqueous Solutions using Optical Subtraction’’, Proc. SPIE, **4624**, 2002 pp. 150-159.

Oral presentation at the Pittsburgh conference 2002 in New Orleans LA: Peter Snoer Jensen and Jimmy Bak, ´´Optical Subtraction Fourier Transform Near Infrared Spectroscopy on Aqueous Solutions’’.

Oral presentation at the Pittsburgh conference 2003 in Orlando FL: Peter Snoer Jensen, Jimmy Bak, Søren Ladefoged and Stefan Andersson-Engels, ´´On-line measurement of trace components in dialysate with dual-beam FT-IR spectroscopy’’. Accepted.

1. Introduction

Water is *the* biological solvent. Indeed, life itself is not possible without it.[1] This may be explained by the abnormally large dielectric constant of water which gives it a striking ability to dissolve ionic substances.[2] Determination of trace components in aqueous solutions is desirable in many diverse applications such as biomedical diagnostics, dairy industry and waste water analysis. All of these applications demand increasing accuracy and reliability, faster answers, simple sample handling and, if possible, non-invasive and non-destructive measurement. The usual chemical analysis does in many cases provide high accuracy and reliability but fails to satisfy the other demands.

Methods based on infrared spectroscopy has the potential to satisfy the demands that chemical analysis does not. Infrared spectroscopy probes the vibrations of the functional groups of molecules by letting infrared light interact with the sample under investigation. This is a non-destructive, and possibly non-invasive, method which is, in principle, capable of identifying and quantifying organic molecules. Each organic molecule has a unique infrared spectrum, and the strength of this spectrum is proportional to the concentration of the molecule. This means that simultaneous determination of several trace components from one spectrum is feasible provided that the spectra are sufficiently different in the spectral regions that are accessible. Unfortunately, the water in aqueous solutions absorbs strongly in the infrared spectral region because of its high concentration. The signals of interest from the trace components are small in comparison and must be extracted from this strong and varying background.

This thesis treats some important aspects of this problem which relates to the fundamental properties of water itself and to the instrumentation used for infrared spectroscopy of aqueous solutions. This thesis is based on work carried out at Risø National Laboratory, Optics and Fluid Dynamics Department, Denmark. It has been largely experimental and has aimed to produce results of general utility and to take advantage of these results in specialized cases as well. This thesis consists of five original scientific papers and the present summary that describes the field to which these papers contribute. This summary makes no attempt to completeness; references to the literature are provided for that purpose. Material contained in the original scientific papers is only minimally duplicated here.

Historically, mid infrared spectroscopy has been used primarily for identification of pure substances in organic chemistry. The arrival of minicomputers, the HeNe gas laser, and the fast Fourier transform in the 1960's made the Fourier transform infrared (FT-IR) spectrometer practical. It became the instrument of choice because it improves signal-to-noise ratio by orders of magnitude compared to a

grating instrument.† At about the same time multivariate methods for analysis of spectral data with many independent overlapping variations found applications in the chemical field. These methods have made quantitative analysis practical in situations where simple measurements of peak heights to determine concentrations are impossible because the peaks are masked by other variations in the spectra that are comparable or much larger. Since then improvements in instrumentation, and the huge progress in data processing capability caused by the increased capability of electronic computers and resulting progress in the development of algorithms for numerical analysis has had tremendous impact. Applications of mid infrared spectroscopy for quantitative analysis of substances has had large success in gas analysis where spectral lines are sharp and isolated, and the background transparent. The use of near infrared spectroscopy has emerged since the 1970's as a technique for on-line monitoring and process control that is now widely used.[3] Within the biomedical field, vibrational spectroscopy is emerging as a potential diagnostic tool with many diverse applications.[4] The increasingly prevalent disease diabetes mellitus has created a demand for continuous non-invasive monitoring of blood glucose concentration. Therefore, methods to do so based on a variety of techniques, including near and mid infrared spectroscopy, has been sought intensively in latter years.[5-15] The arrival of FT-IR microscopes for multi-spectral imaging of tissue has spawned considerable research to characterize cancer from infrared spectra in the hope that pathologists may be given an objective tool for diagnosis.[16-19]

In the research related to the application of infrared spectroscopy for the measurement of trace components in aqueous solutions, much effort has gone into the development of multivariate techniques and the application of these techniques on model systems. Most of the work presented in this thesis investigates the possibility of obtaining the best possible measurements in a given spectral region by consideration of the limitations imposed by the water and the used instrumentation. The motivation for this approach may be found in the huge success of the multivariate methods that have reached a level where only marginal further improvements may be expected. Another motivation may be found in the prevalent optimization methods within this field that are frequently based on results from chemometric calibration experiments. The conclusions reached from such experiments are frequently disregarding the influence of the water absorption spectrum or conditions imposed by the instrumentation. Rather, data are regarded as isolated quantities with the result that misleading conclusions are formed. The standard Fourier transform spectrometer is almost exclusively used for accurate measurements of spectra of aqueous solutions. Part of this thesis

† This improvement is a result of the so-called Fellget, Jaquinot, Connes, and resolution advantages that are discussed in section 3.3.

investigates the possibility of improving this instrument by operating it in a dual-beam, optical null mode. Within the biomedical field, the determination of trace components in spent dialysate from treatment of patients with renal defects is of diagnostic value. This thesis presents measurements of three key components, namely urea, glucose, and phosphate, with the purpose of quantifying these molecules on-line during the treatment of patients and thereby eliminate the need for a traditional analytical chemical analysis. On-line quantification of urea concentrations has been carried out during the treatment of patients with the dual-beam, optical null, instrument.

The present summary will briefly explain the fundamental principles of infrared spectroscopy. Then follows a description of the standard Fourier transform spectrometer. The advantages, limitations and applications of dual-beam, optical subtraction Fourier transform spectroscopy is then described. Having presented the fundamental physics and instrumentation, a description of the principles of quantitative analysis, and multivariate analysis is given. After this discussion of the methodology and techniques found in this field, a discussion of the the absorption properties of water is presented. A discussion of the measurement of trace components in aqueous solutions follows. Lastly, a general description of renal diseases and the treatment of patients by haemodialysis is given. The importance of monitoring the treatment is stressed and the motivation for applying FT-IR spectroscopy to do so is given.

2. Infrared Spectroscopy

This chapter gives a brief overview of the most basic concepts of infrared spectroscopy. Standard references are the books by Colthup, Daly, and Wiberley,[20] and Pavia, Lampman, and Kriz.[21]

In a simple model of a molecule, one finds that the bond strength in molecules and their mass determines the resonant frequencies at which vibrations are exited and light is absorbed. In the simplest description, two atoms in a bond are regarded as a simple harmonic oscillator with resonant frequency in wavenumber units†

$$\bar{\nu} = \frac{1}{2\pi c}\sqrt{K/\mu} \tag{2.1}$$

where K is the force constant, $\mu = m_1 m_2/(m_1 + m_2)$ is the reduced mass of the two molecules with masses m_1 and m_2, respectively. Typical atomic masses are 1, 12, and 16 atomic mass units (exemplified by the H, C and O atom, respectively) and bond strengths are 8.5, 4.5 and 16 N/cm (exemplified by the CH bond, the OH bond in H_2O and the CO bond in CO_2, respectively)[22] Therefore, resonant frequencies lies in the infrared part of the electromagnetic spectrum from $4000 - 500\,\mathrm{cm}^{-1}$ ($2.5 - 12\ \mu$m). Stretching, bending and even more complicated vibrational modes, including several atoms in a molecule, may be excited. Stretching vibrations have large force constants and exists in the high wavenumber region, whereas bending vibrations have comparatively smaller force constants and exists in the low wavenumber regions. In addition, overtone and combination bands may be excited because of anharmonicity of the vibrations, such that light with higher frequencies may exite these vibrations. For a vibration to be infrared active, it must cause a change in the dipole moment of the molecule.[20] Therefore, vibrations around a center of symmetry are not infrared active.‡ For molecules in the gas state, fine structure of absorption bands arise from the different rotational states. Molecules in the liquid state interact so frequently by collisions that absorption bands are broadened. Molecules in the solid state are locked such that peaks are more distinct than in the liquid state. The infrared spectrum of a given molecule provides information about the functional groups present in it and may be used to identify the molecule. The concentration of a given molecule may also be determined, see chapter 5. Interestingly, the thermal radiation from matter at temperatures from room temperature to 800 K has it's maximum between 2200 and $500\,\mathrm{cm}^{-1}$. The maximum moves towards higher frequencies as the temperature is increased. Therefore, infrared spectroscopy is also

† The wavenumber unit cm^{-1} is commonly used in infrared spectroscopy. It is the frequency of the radiation divided by the speed of light c. To convert wavenumbers in cm^{-1} to wavelength in μm divide 10^4 with the wavenumber.

‡ In contrast, the Raman effect, which is inelastic scattering of radiation, requires a change in polarizability and therefore a change in the induced dipole moment.

used for measurements of temperature, determination of spectral emissivity, and remote sensing.

3. Fourier transform infrared spectroscopy

Fourier transform infrared (FT-IR) spectroscopy is today the standard technique for quantitative measurements of infrared spectra. The key concepts of this technique are presented in this chapter as an introduction to the field. The purpose is to supply the reader with a basic understanding of the technique and present it's possibilities and limitations with a special emphasis on the applications relating to measurements of aqueous solutions. Fourier transform infrared spectroscopy is a vast subject. The short description presented here is based on material from the texts by Griffiths and de Haseth[23] and Hirschfeld[24] to which the reader is refered for further details.

3.1. Basic working principle

The Fourier transform infrared spectrometer is basically a Michelson interferometer with a broadband light source, a detector, and an accurate control of the mirror displacement. A schematic drawing is shown in Fig. 3.1. The intensities of the beams for a monochromatic ligth source with unit intensity, the optical pathlength difference, ϕ, and the beamsplitter reflectance and transmittance coefficents R and T are illustrated in the figure.† The mirror displacement is controlled by measuring the zero-crossings of the interference signal from a HeNe laser also passing through a Michelson interferometer. Several different practical realizations of this instrument are possible and commercially available. The one we have used is implemented with corner-cubes instead of flat mirrors as shown in Fig. 3.2. Again the intensities of the beams are illustrated for a monochromatic light source of unit intensity. The arrangement with corner-cubes has two advantages. Firstly, the corner-cubes reflect light 180° regardless of the angle of the incoming light making the configuration immune to tilts of the mirror. Secondly, the corner-cubes separate the incoming and outcoming ray, making the use of two inputs and two outputs of the interferometer practical.

The FT-IR spectrometer measures an interferogram h_n, which is an array of discretely measured points, containing the AC variation of the intensity at the detector as a function of the displacement of the movable mirror. This interferogram. is converted to an intensity spectrum of the light by Fourier transformation as explained in section 3.2.

Because of the high accuracy of the mirror position, determined by the interference signal of the HeNe laser, multiple scans may be co-added such that a linear averaging of the signal may be carried out. In principle, this allows improvement of the signal-to-noise ratio with the square root of the number of scans. The maximum displacement of the movable mirror determines the spectral resolution

† The optical pathlength difference is two times the mirror displacement.

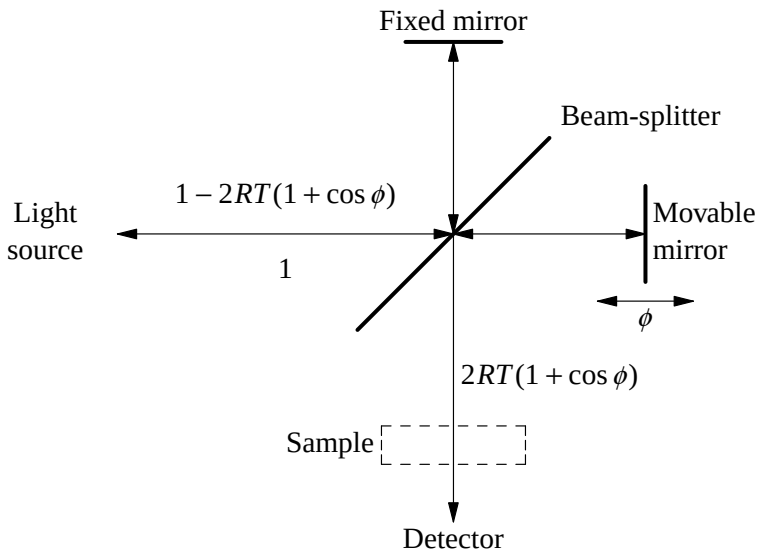

Figure 3.1: Schematic drawing of Fourier transform infrared spectrometer. The intensity of the beams are sketched for a monochromatic light source of unit intensity.

of the spectrometer.

3.2. Calculation of single-beam spectrum

For an ideal beamsplitter with no absorption, equal transmittance and reflectance coefficients $R = T = 0.5$, and a monochromatic light source with intensity p_1 at wavenumber $\bar{\nu}$, the intensity P_1, measured at the detector as function of the phase shift $\phi = 2\pi\bar{\nu}\gamma$ at an optical pathlength difference of γ is given by

$$P_1 = 0.5\,p_1(1+\cos\phi). \tag{3.1}$$

The AC variation of this signal is known as the interferogram. It is a cosine function with period determined by the wavenumber of the incoming light. For a broad-band light source, the measured signal is a superposition of the cosine functions belonging to each wavenumber. The relation bewteen the interferogram and the spectrum of the light source is therefore ideally a cosine transform. In practice, the interferogram is never completely symmetric and it therefore also contains sine components.

The measured interferograms in this thesis have all been double-sided, that is symmetrical around the zero pathlength difference point. An example interferogram is shown in Fig. 3.3. They have been converted into single-beam intensity spectra as shown in the flowchart Fig. 3.4. First the mean of the interferogram is subtracted. Then, the interferogram is apodized by multiplication with a window

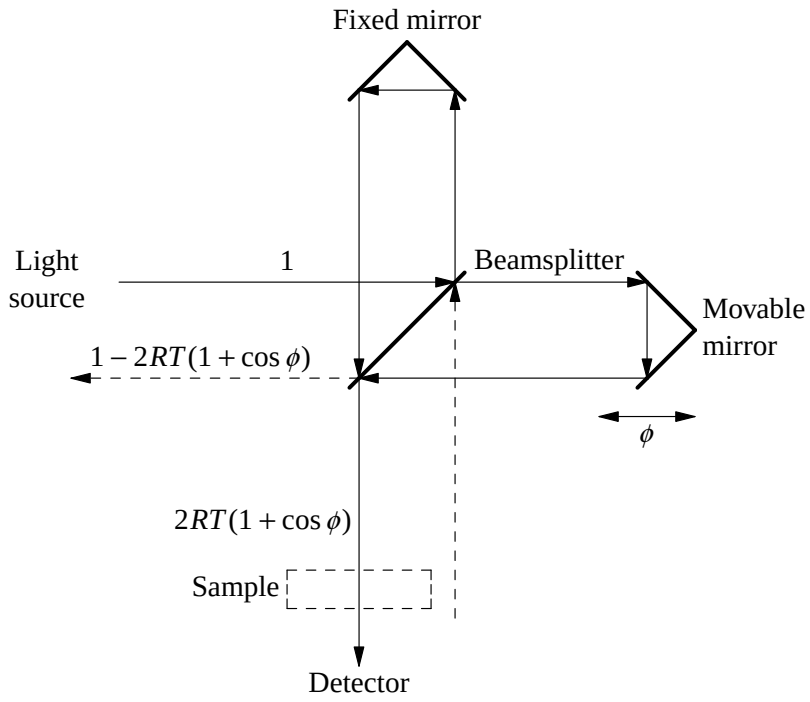

Figure 3.2: Schematic drawing of Fourier transform infrared spectrometer with corner-cube mirrors. Dashed lines show second input and output. The intensity of the beams are sketched for a monochromatic light source of unit intensity.

function. This apodization function is zero at the endpoints of the interferogram and one in the center. It's purpose is to make the interferogram zero at the ends, such that discontinuities are avoided. Many different apodization functions exists.[23, 25, 26] They differ in the tradeoff between reduction of sidelobes, and resolution of the spectrum. The interferogram is then zero-filled by an integer power of two if a spectrum with artificial higher resolution is desired.† The interferogram is then optionally rearranged by splitting it in two halves and exchanging them. This rearrangement is in principle not necessary. It merely shifts the phase by making the interferogram symmetrical around the first array element. The interferogram is then Fourier transformed using the relation

$$H_n = \sum_{k=0}^{N-1} h_k e^{2\pi i k n/N}. \tag{3.1}$$

† The tails of the double sided interferogram is extended with a number of zero's mimicking a spectrum measured with a higher maximum mirror displacement and therefore a higher spectral resolution. But as the added values are nothing but zero's, no additional spectral information is obtained. The result is an interpolation in the spectral domain under the assumption that no higher resolution components than those in the measured interferogram are present.[26]

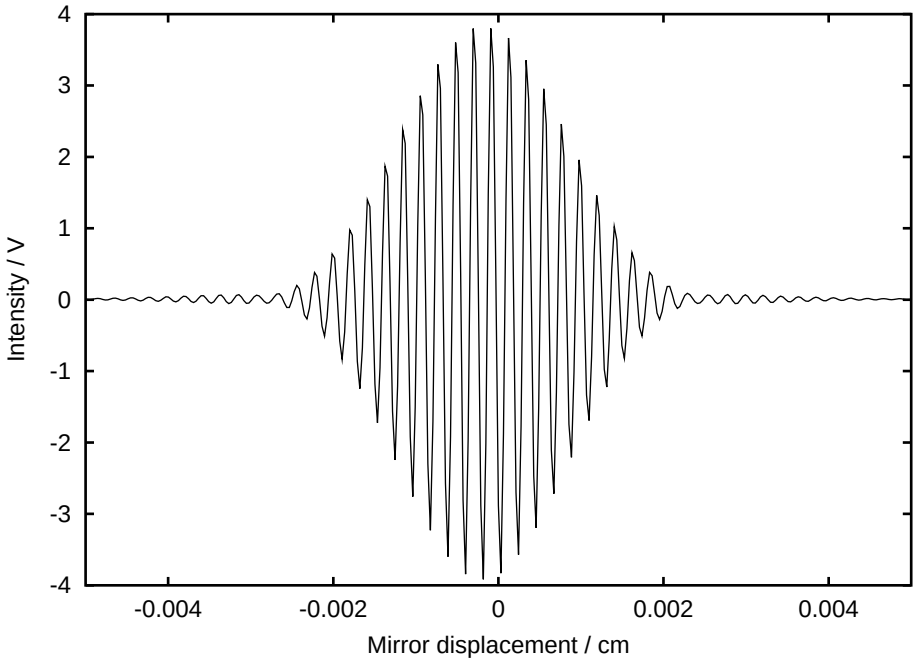

Figure 3.3: Central part of interferogram measured at 32 cm^{-1} resolution through 1 mm of water using a Peltier cooled InAs detector. Short wavelengths has been removed by a long wave pass filter with cutoff at 5000 cm^{-1}. The single beam spectrum resulting from data processing of this interferogram is shown in Fig. 3.5.

In practice this is implemented using the fast Fourier transform (FFT) algorithm.[26, 27] The inverse relation is given by

$$h_k = \frac{1}{N} \sum_{n=0}^{K-1} H_n e^{-2\pi ikn/N}, \tag{3.2}$$

where H_n is the complex array containing the Fourier transform of h_n This Fourier transform is a function of wavenumber $\bar{\nu}$. There is no universal agreement as to the sign in the exponent of the forward and inverse Fourier transform, nor to the distribution of the normalisation constant $1/N$.[26] The measured interferogram is real. Consequently, the values at negative frequencies are the complex conjugates of their positive counterparts. Therefore, time and storage may be reduced by a factor of two by using a special implementation of the discrete Fourier transform.[27] The phase spectrum $\Phi(\bar{\nu})$ is then calculated as

$$\Phi(\bar{\nu}) = \mathrm{atan}(\mathrm{Im}(\bar{\nu})/\,\mathrm{Re}(\bar{\nu})), \tag{3.3}$$

where Re($\bar{\nu}$) and Im($\bar{\nu}$) are the real and imaginary parts of H_n, respectively, with index n corresponding to $\bar{\nu}$.

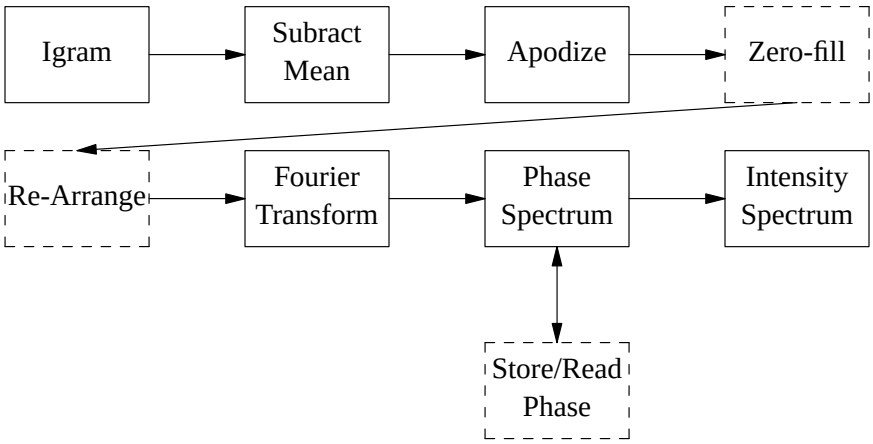

Figure 3.4: Flowchart describing the data processing of interferograms. Dashed boxes are optional.

The calculation takes into account the sign of the nominator and denominator, thereby mapping the angle correctly onto the full unit circle.† From this phase spectrum, the intensity spectrum $I(\bar{\nu})$ is calculated as

$$I(\bar{\nu}) = \mathrm{Re}(\bar{\nu}) \cos \Phi(\bar{\nu}) + \mathrm{Im}(\bar{\nu}) \sin \Phi(\bar{\nu}). \tag{3.4}$$

This procedure has two advantages compared to the nearly equivalent calculation of a power spectrum as

$$P(\bar{\nu}) = (\mathrm{Re}(\bar{\nu})^2 + \mathrm{Im}(\bar{\nu})^2)^{1/2}. \tag{3.5}$$

In the power spectrum, $P(\bar{\nu})$, noise will always give a positive contribution, while noise in the intensity spectrum, $I(\bar{\nu})$, contributes with both positive and negative values.[25] The calculation of the intensity spectrum also makes it possible to substitute a phase calculated from another interferogram. This is necessary in dual-beam applications, to be described in chapter 4, where the phase of the dual-beam spectrum is poorly determined because of high nulling ratio, finite resolution, and resulting leakage of information between neighboring points in the spectrum.[28] The intensity spectrum resulting from this processing of the interferogram from figure 3.3 is shown in figure 3.5.

Physically, the phase does not depend on the light intensity entering the interferometer. The phase is a wavenumber dependent property of the interferometer and

† The standard function atan2(x,y) in C and FORTRAN is designed for this purpose.

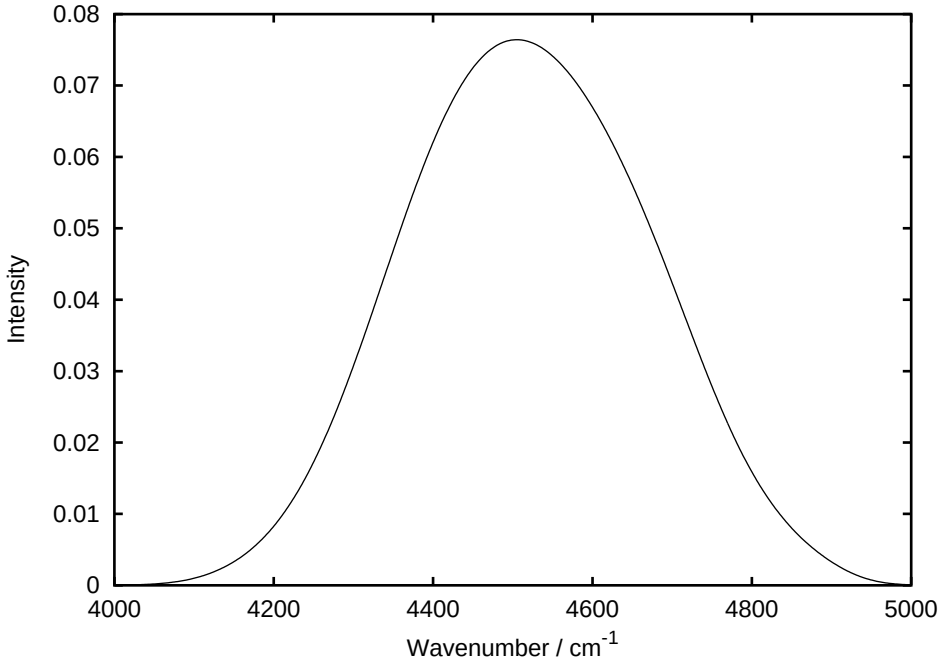

Figure 3.5: Single beam spectrum resulting from data processing of the interferogram shown in Fig. 3.3.

the electronic circuits in the detector system. The interferometer begins where the light reaches the beamsplitter and ends at the detector where the light is measured. By fundamental theorem of Fourier analysis, the phase may be shifted by a time displacement of the measured signal,[26] such that the absolute value also depends on any rearrangement of the interferogram prior to Fourier transformation. Figure 3.6 shows the single-beam spectra and the phases calculated from interferograms measured with a reference blackbody set at temperatures 400 °C and 900 °C. We see that, apart from noise, the two phase spectra are identical and the phase does not depend on the intensity distribution. Notably, the different intensities of the water absortion bands between 4000 and 3500 cm^{-1} does not influence the phase spectra.

Other methods of calculating the intensity spectrum exists of which the Mertz method, and to a lesser degree the Forman method, has become the standards.[29] So standard, in fact, that the effects of phase correction, resolution, apodization and other parameters are almost always discussed in terms of these methods.[28, 30] The Mertz method uses a shorter symmetrical double sided interferogram to calculate a low resolution phase spectrum. The intensity spectrum is then calculated from Eq. 3.4 with values of the phase that have been obtained by interpolation in

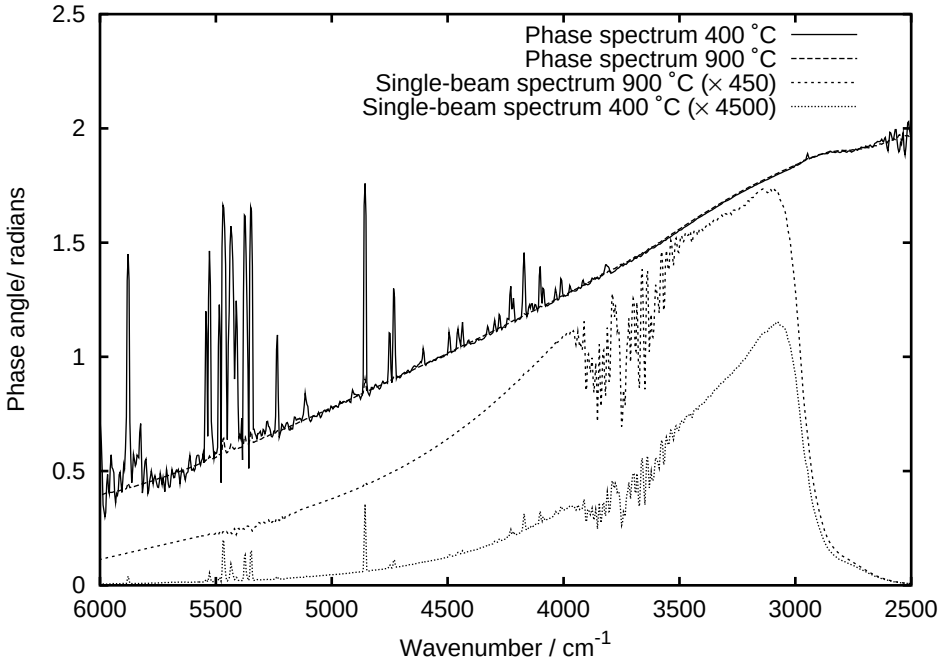

Figure 3.6: Single-beam (in arbitrary units) and phase spectra of single-beam measurements of a reference blackbody set at temperatures 400 °C and 900 °C.

the low resolution phase spectrum. There are two main advantages to this. Firstly, the resolution of the interferogram may be increased while storing the same number of points by measuring an asymmetrical interferogram with a larger maximum retardation. Secondly, the computational burden is smaller because of the smaller number of calls to the atan function. Today, however, these advantages are diminished by todays computers. There are disadvantages to the use of these methods which are caused by the asymmetry of the single-sided interferogram and the interpolation in the low resolution phase spectrum.[28, 30] The procedure where a full phase correction is used on a double-sided interferogram should provide the most accurate results[25] and is critical in situations where differential spectra are measured.[28] For these reasons, single-beam spectra have been calculated using full phase correction. The measurement of an asymmetrical interferogram could still be preferable in special applications. One could think of situations where only a single scan pr. measurement is possible. Measurements at very high resolution, where mechanical considerations with respect to the mirror displacement becomes important and the computational burden large would be another such situation.

3.3. Advantages over grating instrument

The FT-IR spectrometer has replaced the grating instrument because it possesses a number of advantages. These advantages have been discussed by Hirschfeld,[24] Griffiths and de Haseth[23] and others. Here follows a short description of these advantages and some comments regarding their impact on measurements on aqueous solutions.

In a traditional grating instrument, each spectral point is measured sequentially. In contrast, an FT-IR instrument measures all spectral points simultaneously. This results in an improvement in SNR proportional to $\sqrt{N}$ where N is the number of spectral points. This is known as the Fellget advantage. For measurements on aqueous solutions, the spectral range is usually limited to a narrow region selected by the chosen pathlength of the transmission cell and the spectral resolution is chosen to be low because of the broad absorption found in the liquid state. If we assume a spectral range of $1000\,\mathrm{cm}^{-1}$ with a spectral resolution of $16\,\mathrm{cm}^{-1}$ we have an improvement by roughly a factor of eight compared to a grating instrument. A grating instrument with a detector array will also measure all spectral points simultaneously and an FT-IR spectrometer will possess no Felgett advantage over such an instrument.

The absence of a slit in an FT-IR instrument increases it's light gathering power compared to a grating instrument. The light gathering power is usually expressed as the product of the allowed solid angle of the incoming beam and it's cross sectional area and is known as the troughput Φ. The ratio of throughputs in the FT-IR and grating case is given by Griffiths and de Haseth as[23] as

$$\frac{\Phi_\mathrm{F}}{\Phi_\mathrm{G}} = \frac{2\pi A_\mathrm{F}\, fa\bar{\nu}^2}{A_\mathrm{G} h \bar{\nu}_\mathrm{max}}\,, \tag{3.6}$$

where index F refers to the FT-IR instrument and G to the grating instrument A is the area of the mirror / grating, f is the focal length of the grating instrument h is the slit height and a the grating constant. This advantage is seen to be largest at high wavenumbers, it is commonly known as the Jaquinot advantage. The Jaquinot advantage is reduced in cases where sensitive cooled detectors are employed. In these cases, it is commonly necessary to reduce the intensity reaching the detector to avoid saturation.

Wavenumber determination is accurate through the fringe determination of the HeNe laser. This not only means that high resolution spectroscopy is possible, but also allows co-addition of spectra such that the signal to noise ratio may be improved by the square root of the number of scans. This reproducibility of the wavenumber scale is also important when weak absorption on a large background is to be detected. This advantage is known as the Connes advantage.

The resolution of an FT-IR spectrometer depends only on the mirror displacement which may be accurately determined. The larger the displacement the higher the spectral resolution. This advantage is of less importance in spectroscopy of aqueous solutions, where the required spectral resolution is low.

3.4. Limitations of FT-IR spectrometers

The FT-IR spectrometer is an instrument, which is capable of achieving extraordinarily high signal-to-noise ratios. Even so, there are disadvantages to this technique that become important when the ultimate performance of these instruments required. An elaborate discussion of instrumental effects in FT-IR spectroscopy is given by Hirschfeld.[24] This includes effects of mirror displacement from sampling points, double modulation of radiation, emission from the detector and other effects.

Many instrumental effects become serious because the measurement of an absorbance spectrum with an FT-IR spectrometer is a two stage process.† First a reference spectrum $I_0(\bar{\nu})$ is measured and then a sample spectrum $I(\bar{\nu})$. The temporal difference between the two measurements means that the instrumental variations are not necessarily eliminated, and one is left with a signal where one has payed for stability, by accepting increased noise, without receiving it.‡ Such instrumental variations may happen on timescales smaller than the time required for a single scan, such that it is impossible to measure a satisfactory reference. The co-addition of interferograms to reduce noise also means that the temporal difference between the measurement of sample and reference increases. Secondly, the measurement of a small signal riding on top of a large signal is always undesirable because small changes in the large signal may be comparable to the small signal one measures. Thirdly, the finite dynamic range of the analog-to-digital converter means that the digitization of a signal with a large dynamic range of which the relevant information is stored in only very few bits is undesirable. In the case where detector noise is sufficiently low and the intensity reaching the detector sufficiently high, the large dynamic range may even result in a situation where signal-averaging by co-addition of sequential scans does not improve signal-to-noise ratio because the noise is smaller than the distance between two bits on the analog-to-digital converter. In this case one speaks of digitization noise.[23] § In on-line applications, the ideal optical sensor is small

† Grating instruments are usually dual-beam instruments with a chopper that alternates a beam through a sample and reference such that a modulated signal is measured at the detector. In this fashion, the spectrometer measures the transmittance of the sample directly.

‡ When analysis is based on single-beam spectra, such variations are not even sought to be compensated in the measurement process.

§ The application of dual-beam FT-IR spectroscopy attempts to remove these prob-

with no moving parts, cheap and simple. In contrast, the FT-IR spectrometer is large, expensive and complicated.

3.5. Sources in IR and NIR

The most commonly used light source used in the mid infrared region is a SiC globar. This is a rod, heated to a temperature of about 800 °C by a current passing through it, which emits thermal radiation with a maximum intensity at approximately 2100 cm^{-1}. In the near infrared region, quartz halogen tungsten filament lamps, are usually employed. They have a temperature of about 2500 °C providing maximum intensity at 5500 cm^{-1}. The absorption of quartz in the mid infrared region prevents application of this light source in that spectral region.

3.6. Detectors in IR and NIR

The standard detector in most FT-IR instruments is the deuterated triglycine sulphate (DTGS) detector. This is a thermal detector, a so-called pyroelectric bolometer, that consists of a ferroelectric crystal which has a Curie point close to room temperature. The crystal therefore exhibits large changes in electrical polarizability when exposed to modulated radiation. By placing electrodes on the crystal faces, the crystal acts as a capacitor across which an AC voltage may be measured. This detector is very linear, stable, and has a wide spectral range of operation.

Semiconductor based quantum detectors are used when increased sensitivity and low noise is required. In the mid infrared spectral region, the mercury cadmium telluride (MCT) detector is almost exclusively used. This detector usually requires cooling by liquid N_2. In the near infrared spectral region InSb and InAS detectors are employed. These detectors may be liquid N_2 or Peltier Cooled. Compared with the DTGS detector, these detectors have lower noise, higher sensitivity, but a narrower spectral range of operation. The levels of intensity they may be exposed to is far lower than the ones the DTGS accept. The MCT detector in particular has a non-linear behavior when exposed to too high levels of intensity.

The difference in linearity between the mid infrared MCT detector and the near infrared InSb and InAs detectors may be understood from the structure of these detectors. These detectors are constructed to be sensitive to different energy levels of radiation. In a semi-conductor structure with a conduction band separated from a valence band by a band-gap, a current can be measured when free electron are created in the conduction band by absorption of photons with energies greater

lems related to dynamic rang by a simultaneous measuerent of the difference between sample and reference. The technique is described in chapter 4.

than the band-gap. A mid infrared detector has a small band-gap as it is required to detect radiation with low energies and thermal excitation creates a considerable number of electrons in the conduction band, even when the detector is cooled. The reservoir of electrons that may be excited by the incoming IR radiation is therefore small. This is illustrated in figure 3.7. With too much light intensity reaching the detector, the reservoir is dried out and the detector saturates.

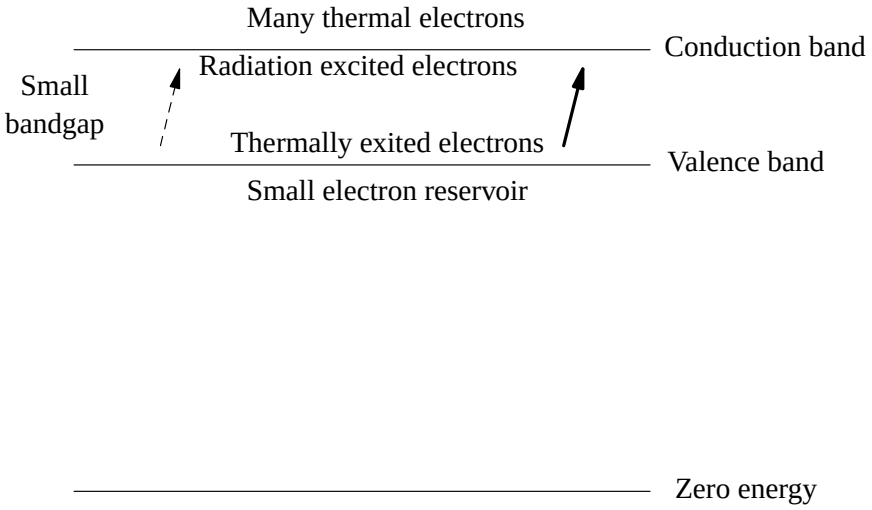

Figure 3.7: Bandgap properties of mid infrared quantum detectors.

A near infrared detector is required to detect much higher energies and, consequently, it has a much larger band-gap. For this reason, thermal excitation does not create as many electrons in the conduction band. A higher incident flux of radiation is therefore permissible before saturation sets in. This is illustrated in figure 3.8. The use of dual-beam techniques where the intensity reaching the detector is twice as high as in the single-beam case is therefore much more limited by the MCT detector in the mid infrared region than by the InAs detector in the near infrared region. A thorough discussion of infrared detectors is given by Kinch.[31]

3.7. Infrared windows

The window materials used as in FT-IR spectrometers and sample accessories must be transparent to infrared radiation. The most common infrared windows are salts that are hygroscopic and therefore ill suited for use in connection with aqueous solutions. Most beamsplitters consists of a base of such a material with a coating and FT-IR spectrometers are therefore either sealed, with a dessicating material within, or purged with dry air, free of water and carbon dioxide. These two gasses have intense infrared absorption bands and the purge also has the

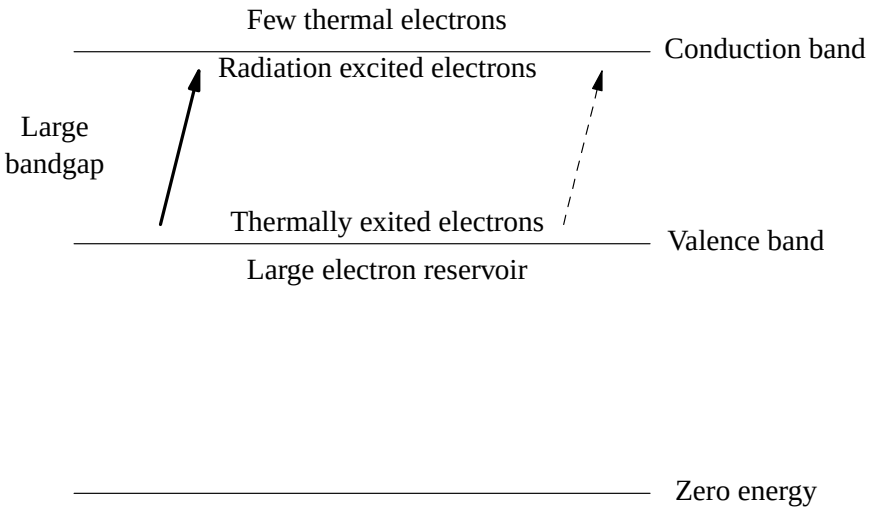

Figure 3.8: Bandgap properties of near infrared quantum detectors.

purpose of reducing the concentration of these two gases. The most commonly used window material for measurements on aqueous solutions is CaF_2 which is only very weakly dissolved by water and has an index of refraction which is close to that of water. Another commonly used material is ZnSe which has a higher index of refraction but is soft. In the near infrared spectral range, quartz and sapphire windows may be employed. They have the advantage of being hard and chemically inert. A table of infrared materials is shown in Table 3.1.

Material	Spectral range cm^{-1}	Refractive index at $1000\,cm^{-1}$	Water solubility g/100g
KBr	48800 – 345	1.52	53.5
NaCl	52600 – 457	1.49	35.7
CaF_2	79500 – 1111	1.39	0.0016
ZnSe	15000 – 461	2.4	insol.
Sapphire	40000 – 1608	2.6	insol.
Suprasil 300®	57142 – 2857	2.5	insol.
Diamond	30000 – 30	2.4	insol.

Table 3.1: Properties of infrared window materials. The spectral range is given for a window thickness of 1 mm, except for Suprasil, where the thickness is 10 mm. Data from Pike Technologies, Madison WI, USA, Catalog 2001.

3.8. Sampling techniques

The measurement of an absorption spectrum of an aqueous solution is mainly carried out using two different sampling techniques, namely through the application of a transmission cell or an attenuated total reflection (ATR) cell.[32] In this work, the use of an ATR cell has been limited to preliminary investigations an no ATR spectrum is presented. Even so, the technique is standard, and preferred by many other groups, so a description of both techniques is given. The transmision cell consists of two IR transparent windows between which the aqueous solution is placed. The light ray of the interferometer then passes through the IR windows and the aqueous solution before reaching the detector. This is illustrated in figure 3.9.

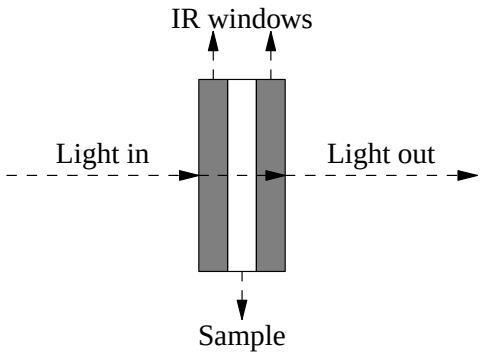

Figure 3.9: Schematic drawing of transmission cell.

Transmission cells are well suited for near infrared spectroscopy of aqueous solutions. In this spectral region optimal pathlengths are in the range $0.5 - 10\,\text{mm}$ and consequently much larger than the wavelength of the light. In the mid infrared region, the pathlength is in the range $7 - 50\,\mu\text{m}$ which is of the same order of magnitude as the wavelength of the light. This means that multiple reflection inside the transmission cell may cause fringe effects in the spectrum in the mid infrared region, but not in the near infrared region.†

The magnitude of this effect increases with the difference between the index of refraction of the sample and of the window material. For an accurate determination of the absolute absorption coefficient of water, it is necessary to correct for the difference in Fresnel reflection at the interfaces in an empty cell and in a water filled cell because the index of refraction of water is dependent on the wavenumber. Instead, one may measure a reference spectrum of a water filled sample, with pathlength δ, and a sample spectrum with a pathlength of $d + \delta$, to

† This effect is normally used to determine the pathlength of a transmission cell. The pathlength is given by $d = (n\Delta\bar{\nu})^{-1}$ where n is the index of refraction of the sample (normally air), and $\Delta\bar{\nu}$ is the period of the fringe pattern in cm^{-1}.

obtain the absorbance spectrum of the sample at pathlength d, thereby eliminating the difference in index of refraction at the interfaces.

Attenuated total reflection is a sampling technique where light passes through a crystal or an IR optical fiber and is totally internally reflected. The evanescent wave reaches into the sample and is altered by changes in the absorption and index of refraction of the sample. This is illustrated in figure 3.10.

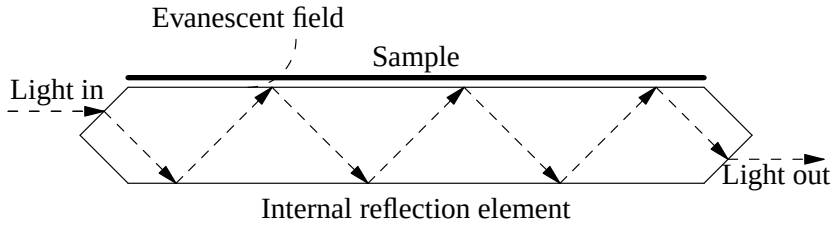

Figure 3.10: Schematic drawing of ATR cell.

This allows absorption spectroscopy with penetration depths comparable to the wavelength of the light. More precisely, the penetration depth, d_p, defined as the depth of $1/e$ attenuation, is given by[23]

$$d_p = \frac{\lambda}{2\pi n_p(\sin^2\phi - n_s^2/n_p^2)^{\frac{1}{2}}} \tag{3.7}$$

where λ is the wavelength of the light, n_p is the index of refraction of the crystal, n_s is the index of refraction of the sample and ϕ is the angle of incidence. This technique has become standard in the mid infrared spectral region where the depth of penetration of a typical ATR cell is close to the optimal. The main advantages compared to a transmission cell consist in elimination of fringe effects present in transmission cells with comparable pathlengths and ease of sample handling. An ATR cell is not recommended in the near infrared region where it's depth of penetration is too small to give a reasonable signal from the analytes. The sensitivity of the ATR technique may be improved by multiple reflection cells. The main disadvantage of this technique is the vulnerability to adsorption onto the ATR cell. For comparison with transmission spectra, the ATR spectra must be corrected for the wavenumber dependent penetration depth[23] and for the the anomalous dispersion of water.[33]

4. Dual-beam Fourier transform infrared spectroscopy

The measurement of weak signals on a strong and varying background is generally considered difficult and the ability of the FT-IR spectrometer to remove a common background by subtraction of a reference from a sample signal in the measurement process leaving only their difference has been suggested early by Fellget.[34] Some nine years thereafter applications of this technique were demonstrated by by Bar-Lev,[35] Low and Mark,[36] Vanasse,[37-39] Griffiths,[40] Chandrasekhar, Genzel, and Kuhl.[41-43] The different variants of this technique are all known as dual-beam FT-IR spectroscopy. Notably, the application of dual-beam FT-IR spectroscopy for measurements on biological samples were suggested by Chandrasekhar, Genzel, and Kuhl as early as 1976.[41] This chapter will describe the principles of dual-beam FT-IR spectroscopy for the two modes of operation known as single-input-double-output and double-input-single-output. The advantages one seeks to obtain compared to a traditional single-beam mode of operation and the subtle differences between the two modes of operation are described. The limitations and difficulties of the dual-beam FT-IR technique are described. A short list of notable previous applications are given that are followed by a motivation for applying this technique for measurements of aqueous solutions.

In dual-beam FT-IR spectroscopy, the symmetry of the Michelson interferometer is taken advantage of to provide either two inputs or two outputs, or both. This is illustrated in Fig. 4.1. The following presentation closely follows that given by Chandrasekhar, Genzel, and Kuhl.[41] Assume two monochromatic light sources emitting radiation at wavenumber $\bar{\nu}$ with intensities p_1 and p_2 placed at input 1 and input 2, respectively. The intensity at at output 1, P_1, will then be

$$\begin{aligned} P_1 = {} & p_1 2RT(1+\cos\phi) \\ & + p_2[(R+T)^2 - 2RT(1+\cos\phi) + 4RT\cos\Phi\cos(\phi-\Phi)] \\ & + 4(p_1 p_2 RT)^{\frac{1}{2}}\cos(\phi/2)\times[R\cos(\Phi-\delta-\phi/2) + T\cos(\Phi+\delta-\phi/2). \end{aligned} \tag{4.1}$$

In this expression, ϕ is the optical phase shift $2\pi\bar{\nu}\gamma$ as in section 3.2, Φ is the phase difference between the reflected and transmitted beams on the beamsplitter, δ is the phase difference of the two input beams, and R and T are the reflectance and transmittance coefficients of the beamsplitter. The corresponding expression for the intensity at output 2, P_2, will be similar. It may be obtained by exchanging p_1 and p_2, and changing the signs of ϕ and δ in Eq. 4.1. These two expressions may be simpified if we assume that the beamsplitter is ideal such that $R = T = 0.5$ and $\Phi = \pi/2$. If we further assume that the two inputs are uncorrelated, the last term in Eq. 4.1 will be rapidly varying and average to zero. One then obtains the following expressions for the intensities at the two outputs:

$$P_1 = 0.5(p_1 + p_2 + (p_1 - p_2)\cos\phi) \tag{4.2}$$

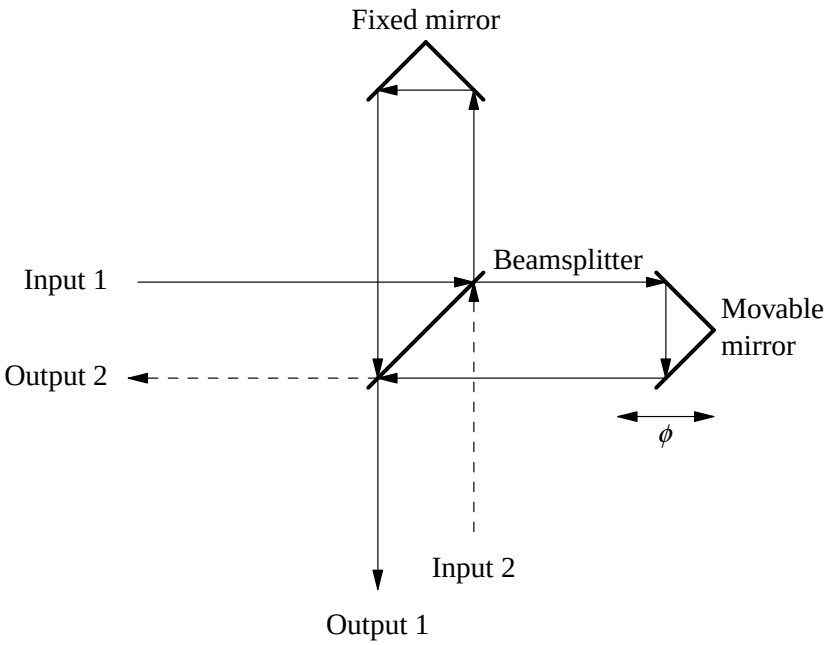

Figure 4.1: Schematic drawing of Fourier transform infrared spectrometer with corner-cube mirrors. Dashed lines show second input and output. The possibility of two inputs and two outputs is shown.

and

$$P_2 = 0.5(p_1 + p_2 - (p_1 - p_2)\cos\phi). \tag{4.3}$$

One observes that the sum of the two output intensities is equal to the sum of the two input intensities and independent of the optical phase shift, ϕ. If the two inputs have identical intensity, both outputs will have zero modulation. If the second source intensity is zero, $p_2 = 0$, Eq. 4.2 reduces to Eq. 3.1 as it should.

4.1. Advantages of dual-beam FT-IR spectscopy

The removal of the background common to the sample and reference forces the signal of interest to emerge from a flat baseline where it is more easily quantified. The dynamic range of the signal is reduced and the full range of the analog-to-digital converter in the spectrometer may be employed to digitize only the signal of interest, excluding the background.† This prevents the spectrometer from being limited in performance by digitization noise as described in section 3.4. Most instrumental variations are common to both inputs and should therefore cancel in the measurement process. The optical subtraction happens on a per-point basis in the interferogram with exact synchronicity and is therefore capable of eliminating variations that takes place on timescales smaller than a single scan.

4.2. Double-input-single-output mode:

If the two inputs have different intensities, one may measure an interferogram at one of the two outputs which contains only the difference between the two inputs. This is essentially the method that has been used in papers I and IV.† In those papers, light is collected from a single source and two beams are passed through each their transmission cell before entering the spectrometer through the input ports. Let T_s and T_r denote the transmittance of the sample and reference cells, respectively, and let $p = p_1 = p_2$ denote the intensity of the common source. Equation 4.2 is then modified to

$$P_1 = 0.5p(T_r + T_s) + (T_r - T_s)\cos\phi. \tag{4.4}$$

The direct difference between the transmittances of the two cells is measured as the AC part of Eq. 4.4. This is known as a double-input-single-output configuration.

4.3. Single-input-double-output mode:

If one uses only a single input, p_1 and passes the two outputs through a sample and a reference cell, respectively, before letting them reach a common detector, one speaks of a single-input-double-output configuration. Denoting the transmittance of the sample and reference, T_r and T_s, respectively, The intensity at the combined output is

$$P_{1+2} = P_1T_r + P_2T_s = 0.5p_1(T_r + T_s) + (T_r - T_s)\cos\phi. \tag{4.5}$$

Again, one measures only the difference in transmittance between the two samples.

4.4. Differences between the single-input-double-output and the double-input-single-output configurations.

The expressions Eqs. 4.4 and 4.5 look deceptively alike. There are subtle differences although both methods are described as dual-beam, optical null, optical subtraction FT-IR spectroscopy. Both methods have in common, that a DC component of the measured intensity at the detector is two times that found in the normal single-beam mode of operation of an FT-IR spectrometer. This presents problems with saturation of the normally employed MCT detector in the mid infrared spectral region.[44] In this spectral region, beamsplitter absorption also limits the degree of opticall nulling that may be obtained.[23]

In the double-input-single-output mode of operation, the eigenradiation of the reference and sample is modulated by the interferometer such that sample and

† For obvious reasons, this is also the mode of operation for dual-beam FT-IR remote sensing applications.

reference temperature differences are included in the measurement. The addition of the two beams are simple, because the light in the two beams are uncorrelated, but the technique requires that light with equal intensity and spectral distribution is passed through the sample and reference. The alignment and of the optical components are facilitated by the placement before the interferometer. The use of two inputs also enable a higher total intensity to be measured compared to the use of only a single input.

In the single-input-double-output mode of operation, the eigenradiation of the sample and reference remains unmodulated and contributes only with a DC term on the detector which is not measured. In this mode of operation the sample and reference are part of the interferometer and interference problems may arise. The detector must be sufficiently large to average out interference fringes resulting from this undesired modulation. Another possibility is to measure the light at the two outputs with each their detector and add the signals electronically instead. This procedure reduces the interference problems and minimizes the total intensity reaching a single detector, but is limited by the requirement that the two detectors must have identical characteristics. In this case one speaks of electronic subtraction.

4.5. Earlier applications

The applications have been primarily in the mid infrared region for various measurements of weak absorption in a transparent medium with the background to be eliminated consisting of the source intensity distribution. The early application of Griffiths, Gomez-Taylor, and Kemeny for the determination of trace components in gas chromatography is a good examples of a single-input-double-output experiment.[45, 46] A Later application by Tripp and Hair for the detection of adsorbed polymer monolayers on mica demonstrates that the double-input-single-output mode of operation may be used with advantage for samples at room temperature.[47, 48] The work by Beduhn and White demonstrating the feasability of single-input-double-output with electronic subtraction.[49] In these cases, The non-linear behavior of the MCT detector has limited the use of this technique, because it becomes necessary to reduce the intensity reaching the MCT detector with corresponding decrease in signal-to-noise ratio as a result. As an example Tripp and Hair reported a nulling ratio of a factor of 50 that only translated into an improvement in signal to noise ratio of five because of the non-linear behavior of the MCT detector.

4.6. Advantages in the near infrared for measurements on aqoueous solutions

As described in section 3.6, near infrared detectors accepts a higher incident flux before they saturate. In addition there is no beamsplitter absorption and the eigenradiation of samples at room temperature is small. The measurement on aqueous solutions in the near infrared spectral range requires only a low resolution. The spectral range may be reduced to a narrow range with no loss of information because the optical pathlength and the absorption spectrum of water only allows a high sighnal-to-noise ratio in a narrow region as described in paper II. The absorption of water also helps to reduce the incident flux on the detector. The optimal transmission pathlenght is long compared to those required in the mid infrared region, therefore a couple of transmission cells with equal pathlength is easily constructed. We were curious as to wether these advantages would result in an improvement when the double-input-single-output mode of operation were compared with the single-beam mode. Paper I demonstrates, that one obtains a significant advantage in the combination band $5000 - 4000\,\mathrm{cm}^{-1}$ by measuring with a dual-beam instrument instead of a single-beam measurement. Even though the main variations present in both types of measurements, instrumental variations are eliminated in the dual-beam measurement.

4.7. Differences in computation

As described in section 3.3 the calculation of a dual-beam spectrum from a measured dual-beam interferogram requires the use of a single-beam phase spectrum. Another difference from measurements with a single-beam instrument lies in the calculation of an absorption spectrum from a sample, I, and a reference I_0. As described in chapter 5, the absorbance, A, is given by $A = -\log_{10} I/I_0$. The measured dual-beam spectrum, D, is the difference between the sample and reference $D = I - I_0$. Therefore, the absorbance may be written with good precision as $A = (1/\ln 10) \times (D/I_0)$. We have assumed that D is much smaller than I and used the Taylor expansion for the log function.

5. Quantitative analysis

The concepts of quantitative analysis are presented in this chapter. The interest focuses on the influence of drift and noise as two key factors that determine the success of any quantitative measurement. The advantage of a full spectral measurement, as in FT-IR spectroscopy, to distinguish between these two quantities and the possibilities for reducing their impact on quantitative measurements are discussed.

In quantitative analysis, one traditionally measures the absorbance of a substance to determine a concentration. The absorbance $A(\bar{\nu})$, at a given wavenumber $\bar{\nu}$, is given by

$$A(\bar{\nu}) = -\log_{10} I(\bar{\nu})/I_0(\bar{\nu}) \tag{5.1}$$

where $I(\bar{\nu})$ is a measurement of the sample intensity and $I_0(\bar{\nu})$ is a measurement of the reference intensity. The choice of reference depends on the application. In many cases a reference with no sample present is used. In other cases a reference is chosen which resembles the sample. This issue is disussed in paper II. Most grating instruments measure the ratio $I(\bar{\nu})/I_0(\bar{\nu})$, known as the transmittance, directly, but the Fourier transform instrument measures the sample and reference intensity spectra separately. By taking the ratio of $I(\bar{\nu})$ and $I_0(\bar{\nu})$, one creates a dimensionless number which ideally eliminates all the dependency on the instrument, including spectral intensity distribution of the source and sensitivity of the detector. This is on condition that the instrument remains constant between the measurement of sample and reference. Note, that noise is not eliminated and still depends on the source and detector. The noise is increased because the relevant signal is composed of two measurements, each containing noise. The increase in noise pays for elimination of instrumental effects, including drift.

5.1. Beer's law

Quantitative analysis is based on Beer's law, which states that the absorbance of a substance, at a given wavenumber $\bar{\nu}$, is proportional to the molar concentration c of the substance and the pathlength l:

$$A(\bar{\nu}) = \varepsilon(\bar{\nu})cl; \tag{5.2}$$

where $\varepsilon(\bar{\nu})$, known as the molar absorptivity, is the wavenumber dependent proportionality constant. Beer's law says that the intensity decays exponentially with pathlength and with the concentration of the substance.

Chemometric methods to extract the concentration from a measurement where several components have overlapping signals exists, of which the ones most commonly applied will be discussed in chapter 6.

5.2. Drift, noise, and data pre-treatment

Traditionally drift and influences from instrumental effects have been considered more problematic than noise. In applications where small signals are to be detected, and with the now available methods of data analysis, noise may prove to be more problematic than instrumental effects. If one considers a single point measurement, at a given wavenumber, noise and drift are indistinguishable. If one has available a full spectrum, on the other hand, drift and influences of instrumental variations may be reduced because they have a spectral structure that may be included in the calibration process. Noise, is impossible to remove from a single spectrum because it is uncorrelated from point to point in the spectrum.

Noise may be reduced by averaging a large number of measurements, but the SNR is proportional to the square root of the number of measurements. This strongly limits this procedure because the measurement time becomes prohibitively large.[50] In practice it turns out that many FT-IR instruments fail to signal average well beyond a certain point.[51] The spectrum may be low-pass filtered, which does in a sense remove noise. But such a procedure is based on a priori assumptions about the spectrum, which may not be true, and reduces the spectral resolution of the data. In addition, it is doubtful that such a smoothing represents an advantage in a calibration. Smoothing is probably most justified when used as a graphical technique to guide the eye.[27] High-pass filtering, including derivation, may remove baseline variations, but such a procedure will also remove any broad-band variation which is part of the signal of interest. In general, any data pre-treatment which is carried out to remove drift will result in an increased noise or degraded spectral resolution. Noise therefore ultimately limits the calibration. For this reason, single-beam spectra (or logarithmized single-beam spectra) are also used today in quantitative analysis. In this case, variations and drift are included in the modeling of the data instead of eliminated in the measurement process.[52] The FT-IR instrument has the advantage over the grating instrument in possessing a superior signal-to-noise ratio. In contrast, the dual-beam infrared grating instrument is made to eliminate drift by measuring the transmittance directly. The dual-beam, optical null, FT-IR spectrometer also seeks to eliminate drift in the measurement process, but does so by measuring a difference between two samples instead of a ratio. A dimensionless number is therefore not obtained.

The variability of the sample population also influences the accuracy of any calibration. With a large variability in a sample population, many calibration samples and many independent spectral points will be necessary to maintain stability and accuracy. The variability of the sample population is usually given as an intrinsic part of a job, and reducing a population variability then means to exclude certain classes of samples. This may be necessary, but is seldom desirable.

6. Chemometric calibration techniques

In this chapter, various methods for analysis of spectroscopic data are described. These methods have been used in the original scientific papers as available method without a detailed description. This chapter is thus, on purpose, slightly more extensive than the others providing details not found in the scientific papers.

In traditional statistics, a large number of measurements of a single quantity, or paired quantities, are carried out and used to provide the information of interest. There does exist a large class of experiments, to which spectroscopic measurements belong, where comparatively few measurements of a large number of independent quantities are carried out. To take advantage of such data, a reduction of dimensionality is necessary. This reduction is made possible by the covariance between measured variables. Principal component analysis (PCA),[53] principal component regression (PCR), and partial least squares regression (PLSR)[54] are all methods based on such data reduction schemes. They are, today, the most commonly used data analysis methods used in mid and near infrared spectroscopy for quantitative analysis.

6.1. Principal component analysis

Principal component analysis takes a collection of spectra arranged as a matrix, $\mathbf{X}$, where each row, $\mathbf{X}_i$, is a spectrum, and decomposes this matrix into a product of two other matrices, the score matrix, $\mathbf{T}$, and the transpose of the loading matrix, $\mathbf{P}$, and a matrix, $\mathbf{E}$, such that

$$\mathbf{X} = \mathbf{T} \cdot \mathbf{P}^{\mathrm{T}} + \mathbf{E}. \tag{6.1}$$

The matrix $\mathbf{E}$ is zero if the full dimension of $\mathbf{P}$ is retained. The advantages of the decomposition are obtained only when the dimension of the data is reduced. In this case, the signal is separated from the noise contained in $\mathbf{E}$ as a residual. This decomposition may be viewed as a transformation to another coordinate system, where the new axes, $\mathbf{P}_i$, are the spectra of the variations found in the data set. The new coordinate system is orthonormal and rotated so that the first axis lies in the centre of the data and minimizes the variance when subtracted from the data. The second axis lies in the center of this new data set where the first axis has been subtracted and so on ... † The new set of axes, $\mathbf{P}$, is known as the loadings and the coordinates in this new coordinate system, $\mathbf{T}_i$, are known as the scores.

The principal component analysis is identical to a singular value decomposition

† This is a sketch of the NIPALS algorithm, which is commonly used to carry out the PCA.[54] This method may be employed with minor modifications if data points are missing. This is not an issue when measuring infrared spectra with a Fourier transform spectrometer, however.

(SVD) of the matrix **X** into the product of an orthonormal matrix, **U**, a diagonal matrix, **w**, and the transpose of an orthonormal square matrix, **V**:

$$\mathbf{X} = \mathbf{U} \cdot \mathbf{w} \cdot \mathbf{V}^{\mathrm{T}} \tag{6.2}$$

In this case, the score matrix, **T**, is identical to the product of the matrix **U** and the diagonal matrix **w**. Deletion of principal components representing noise, is then carried out by setting the corresponding small value in the diagonal matrix **w** to zero. Double precision versions of routines from Numerical Recipes in C[27] for singular value decomposition has been used in this work to carry out the principal component analysis. The difference between the two mathematically equivalent formulations is largely conceptual. PCA stresses the graphical interpretation of the data in the transformed coordinate system. The scores (coordinates) may be interpreted to detect outliers and drift and the loadings (axes) may be interpreted as spectra of the primary variations found in the data. These in turn may be identified with physical or chemical variations.

It is customary to center the data matrix **X** by subtracting the mean spectrum $\bar{\mathbf{x}}$ before carrying out PCA. In some applications the data matrix is scaled by division with the standard deviation spectrum, $\bar{\mathbf{s}}$. We have not done that in this work.

As a simple example of this graphical interpretation, PCA on a data matrix consisting of 40 single beam spectra taken with 10 minutes intervals, measured with an empty beam using an MCT detector were carried out. The first measurement was carrried out 10 minutes after filling the detector with liquid N_2. Figure 6.1 shows the first diagonal values **w**. The figure reveals two dominating orthogonal variations in the data set. Figure 6.2 shows the first and second loading vectors $\mathbf{V}_1$ and $\mathbf{V}_2$. The first loading vector is seen to model the sensitivity of the detector which is the broad shape of the baseline Moreover, the contents of H_2O and CO_2 in the empty beam are represented by OH bending vibrations at $2000 - 1400\,\mathrm{cm}^{-1}$, OH stretching vibrations at $4000 - 3500\,\mathrm{cm}^{-1}$ and assymetrical stretch vibrations of CO at $2300\,\mathrm{cm}^{-1}$. There is a covariance between the sensitivity of the detector and the contents of water and carbon dioxide in the measured data set. The two variations are physically independent. There is no causal connection, yet they both vary monotonically with time. Detector sensitivity increases monotonically and H_2O, and CO_2 concentration decrease monotonically. Both variations converge towards som stable value. This means that the two types of variations may not be completely separated. Figure 6.3 shows a score plot of the first and second scores, $\mathbf{U}_1$ and $\mathbf{U}_2$. Each data point represents a spectrum, such that the essential variation of the spectra are represented by two variables. One observes that the detector stabilizes within 1 hour as the single-beam intensity modeled by the first score converges. A much slower convergence is the gradual removal of H_2O and CO_2 by the continuous purge of the

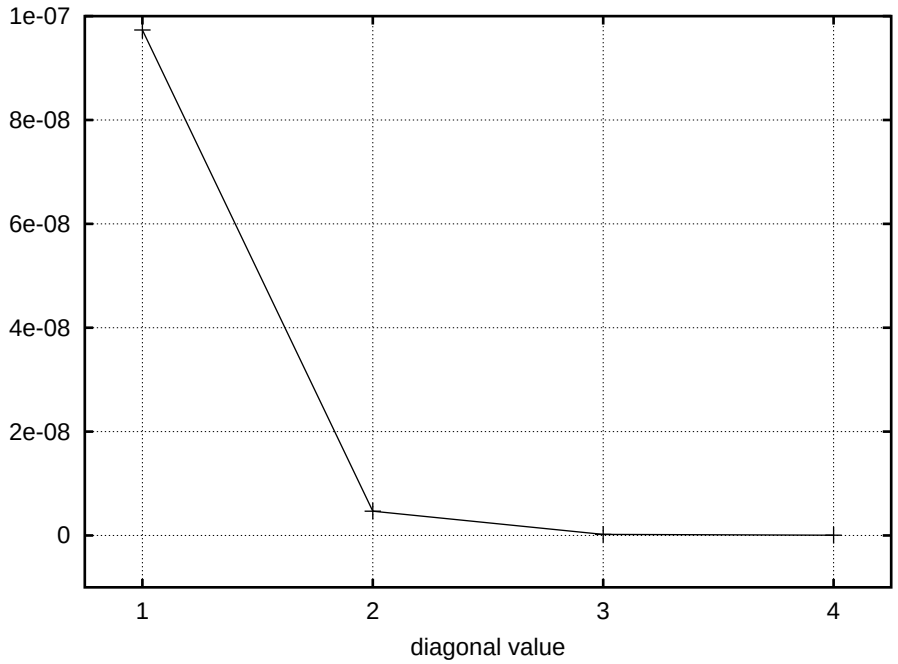

Figure 6.1: Diagonal values from PCA of MCT data.

instrument which is modeled by the second principal component. The third loading vector, which is not shown, contains information related to CO_2 alone. The rest of the loading vectors contains noise and may be disregarded.

6.2. Principal component regression

The orthogonality and reduced dimension of the new coordinate system makes the scores ideally suited for multiple linear regression (MLR) when one wishes to use the spectra for calibration with some control value **y**, typically a concentration, attached to each measured spectrum. Carrying out multiple linear regression on the transformed data set emerging from the principal component analysis is known as principle component regression (PCR).

The result of the PCR calibration is a regression vector, **r**, which depends on the number of principal components that has been retained in the data set. This regression vector, **r**, is then multiplied as a dot product with a spectrum to predict a concentration value belonging to the spectrum.

This is equivalent to finding the best solution, in a least squares sense, to the equation

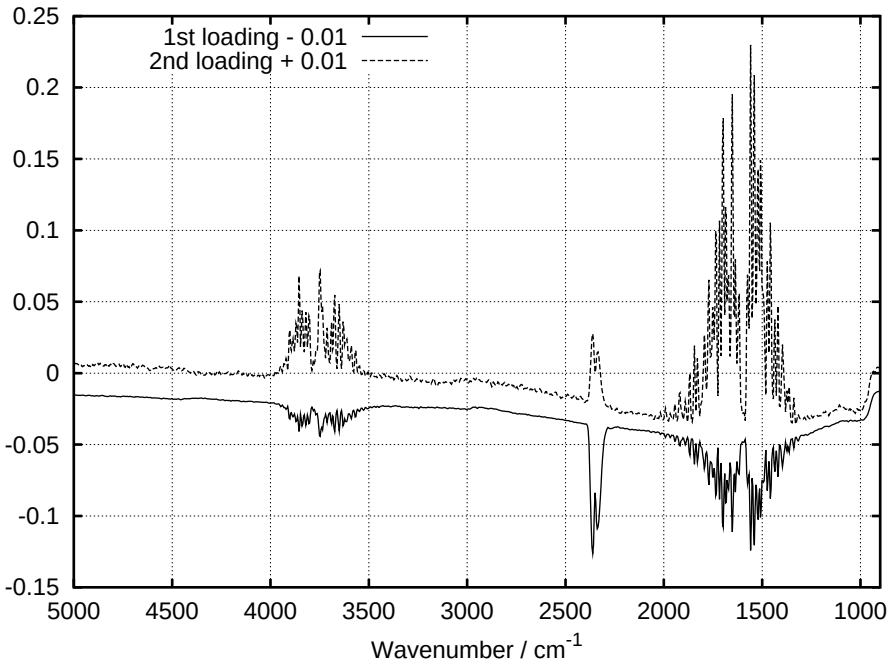

Figure 6.2: First and second loading vectors from PCA of MCT data.

$$\mathbf{X} \cdot \mathbf{r} = \mathbf{y}, \tag{6.3}$$

with the regression vector, **r**, as unknown, by first carrying out the singular value decomposition of **X**, then zeroing the appropriate number of eigenvalues $\mathbf{w}_i$'s and then backsubstituting.[27] Having carried out the singular value decompositon, Backsubstitution is a trivial operation because the matrices **U** and **V** are orthonormal and have their inverses equal to their transposes. The inverse of the diagonal matrix **w** is a diagonal matrix containg the inverses of the elements of **w**. Therefore the regreession vector **r** may be estimated from

$$\mathbf{r} = \mathbf{V} \cdot \mathrm{diag}[1/\mathbf{w}_i] \cdot (\mathbf{U}^{\mathrm{T}}\mathbf{y}). \tag{6.4}$$

This is the method that has been employed in this thesis for PCR.

Having determined the regression vector **r** one may then measure a new set of spectra $\mathbf{X}_{\mathrm{new}}$ and apply Eq. 6.3 to predict the concentrations $\mathbf{y}_{\mathrm{new}}$ of the samples corresponding to these spectra.

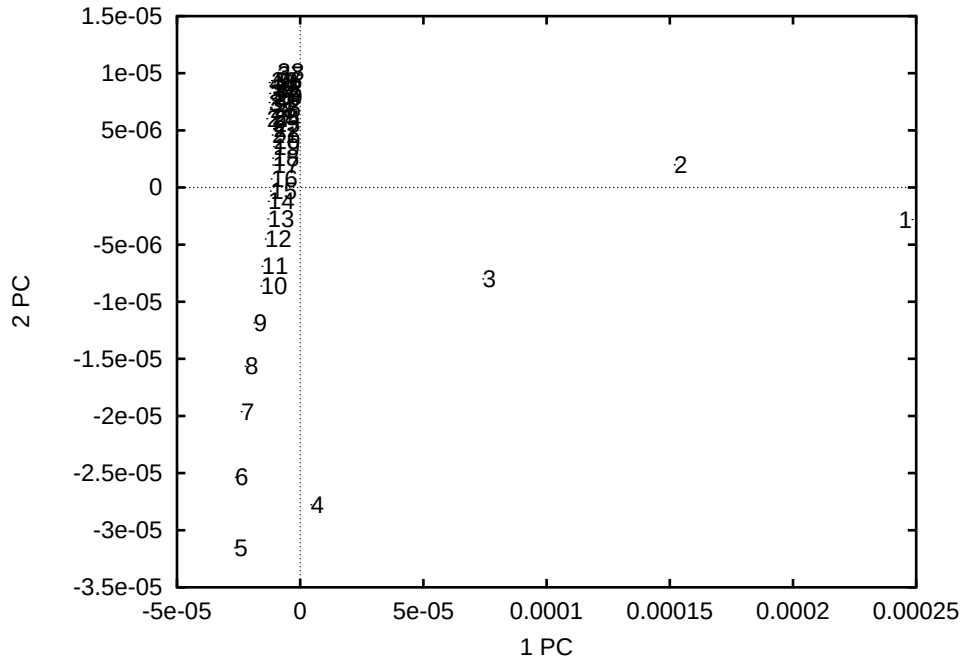

Figure 6.3: Score plot of MCT data first vs. second score.

6.3. Partial least squares regression

Another calibration technique, known as partial least squares regression[54] (PLSR), is also commonly used. This technique takes advantage of the **y** values when transforming the data set, such that spectral variations in **X** that correlates with the variation **y** are selected. In this fashion, signals buried below more dominating irrelevant variations are extracted. This frequently yields simpler models with fewer principal components, now called PLS factors. The price one has to pay for this advantage is that the axes in the transformed coordinate system are no longer orthogonal and that the model is more sensitive to over-fitting.[54, 55] As with PCR, PLSR results in a regression vector **r** which is multiplied with a spectrum as a dot product to obtain an estimate of the concentration value corresponding to the measured spectrum. As a general idea, it is a useful check of the calibration process to use both these methods to construct the regression vector and compare the obtained results. Typically, differences between regression vectors obtained by the two methods is a sign that something unhealthy is going on. Keeping too many components leads to models where spurious correlations cause poor prediction of concentrations belonging to spectra not included in the calibration model. Principal component regression has generally been favored by the author because of the neutral behavior with regard to concentration values and

lack of tendency to over-fit compared to PLSR. For most of the experiments upon which this thesis is based, sample variability is small and the difference between the two methods of calibration is small. The advantages of PLSR does not then emerge, when compared with PCR on the data from these experiments. Even so, both methods of calibration have been applied and results compared, choosing the optimal calibration model as the best of both methods.

6.4. Effect of over-fitting on the regression vector

It is instructive to look at the way the regression vector changes as more and more principal components are included in the model. Typically, the regression vector begins with a broad shape which does not resemble the spectral shape of the control variable it should predict. As more principal components are added, the regression vector resembles the spectral shape of the pure control variable. If interferences are present, the regression vector is then given a lower weight in those spectral regions where the interferences reduce the correlation between the control variable and the data or it is adjusted to compensate for the change caused by the interference. When over-fitting takes place, the regression vector tends to weigh the strongest peak of the control variable and to oscillate in such a way as to average out the spectral values found elsewhere in the spectrum. The multivariate nature of the calibration is reduced and one is left with essentially an univariate model which is much more sensitive to changes in the spectrum that has not been included in the calibration. This is exemplified by the regression vectors for predicting urea concentrations from single-beam spectra presented in Paper I, Fig. 10. By retaining more components, the PLSR calibration will give increasingly accurate prediction of the data upon which it is built. Application of the model to predict concentrations of an independent data set will then result in a large error, often manifested as a bias. This error is caused by a change in spectral structure in the new data set combined with the rapid oscillation and univariate nature of the over-fitted regression vector.

6.5. Influence of signal-to noise ratio on the predictive ability of calibration models.

Given a very accurate regression vector, **r**, from a calibration model based on a large number of samples and a single spectrum from a sample we wish to estimate the concentration of that sample. One may then show, with a simple argument given in paper II, that the uncertainty in the determination of the concentration is proportional to the square root of the number of independent spectral points containing information that correlates with the concentration and inversely proportional to the noise level of these spectral points. The noise level is therefore a stronger factor than the number of independent spectral points, when one wishes to optimize the predictive ability of a model. The number of independent

spectral points is important in the sense that it determines how many independent variations the model can handle and therefore compensate for spectral interferences.

6.6. Validation of calibration models

Clearly, the construction of a calibration model has as its object to predict the concentration of new samples from their spectra. The ability to do so should be verified by testing the calibration model on an independently measured data set.

Testing is frequently done by splitting a measured data set in two nearly equal subsets, constructing the model from one of the two subsets, and predicting the concentrations of the other. If the data set is split in two at random, such that they are intertwined in time, the model will in principle only interpolate when tested on the other part of the data set. This is also the case for cross-validation schemes where the model is constructed repeatedly from parts of the data and tested on the remaining parts. These are the predominant validation methods found in the current literature.

Successful testing of a calibration model is more impressive when the test set is measured at a separate later time, possibly by another person, and even better on a different instrument. In the latter case one speaks of transfer of calibration. If transfer of calibration is possible, the calibration becomes commercially interesting, provided there is a demand for measurements of the control variable, because calibration is an expensive procedure to carry out. This topic currently receives considerable attention.[56] One method is based on calibration on a reference instrument. To make a transfer of calibration possible, the spectrum of a standard sample is measured on this reference instrument. By measuring the spectrum of the standard sample on other instruments and adjusting this spectrum in software to match the one measured on the reference instrument, sufficient similarity of the spectra are obtained to make the transfer of calibration possible.

The calibrations presented in this thesis have consistently been validated from completely independent test sets measured at least one day later than the calibration set.

6.7. Validation measures

The common method of quantifying the quality of the predicted concentrations from a data set is by calculation of the root-mean-square error of prediction, RMSEP, given as

$$\text{RMSEP} = \left(\frac{1}{n} \sum_{i=1}^{n} (y_i - \hat{y}_i)^2 \right)^{\frac{1}{2}} \tag{6.5}$$

where n is the number of samples y are the predicted concentrations and $\hat{y}$ are the corresponding reference values. The same formula may be used to estimate the calibration models internal consistency by applying it to the data upon which it is built. In that case one speaks of the root-mean-square error of calibration, RMSEC. One may further distinguish between systematic errors, most commonly manifested as a bias, and statistical errors. The presence of a bias indicates problems with drift or diffent types of samples in calibration and test set, whereas statistical errors result from noise.

6.8. Chemometry and instrument configuration.

Noise in a given spectral region destroys the possible correlation with a variation in the **y** vector. Therefore PCR and PLSR will create regression vectors that give a high weight to spectral regions with low noise if it contains a correlation with the **y** vector. Paper II demonstrates that the noise level changes strongly with wavenumber for a given choice of pathlength when measurements of aqueous solutions are carried out. Therefore, one may predict in advance, solely from the absorption spectrum of the samples, the spectral regions that will be selected by the regression vector. This was a major motivation for paper II. It is commonly assumed in chemometric analysis, that the noise level in spectral data are roughly identical across a spectrum. Consequently, the results of the analysis are interpreted as intrinsic properties of the samples and not as properties of the instrumental configuration. For chemometric analysis of aqueous solutions, this common assumption does not hold. The noise level depends very strongly on the choice of transmission pathlength, such that the results of the chemometric analysis will be different if this pathlength is changed. In this case it will be necessary to compare the results of the chemometric analysis with the noise levels in the spectra to obtain the correct information of the intrinsic properties of the sample. As pointed out in paper II, the chosen pathlength selects a narrow spectral region where the SNR is optimized. One may therefore profitably optimize this spectral region by filtering out light in the other spectral regions and maximize the intensity in the chosen region. If information in different spectral regions are required, and it is possible to carry out more than one measurement, then one should do so with different choices of pathlength. Interestingly, Hirschfeld has suggested the use of a stepped transmission cell to improve the dynamic range of transmission measurements as early as 1978.[57] The author has seen no other publications where this technique has been applied.

7. The near and mid infrared absorption spectrum of water

Passing from a description of the measurement and data analysis techniques employed in this work, we will now devote our attention to the properties of the measured samples and their influence on possible applications. This thesis is concerned with measurements of trace components in aqueous solutions. The near and mid infrared spectra of such solutions are dominated by the absorption spectrum of water which is described in this chapter. Much information concerning the fysics and structure of water and aqueous solution is contained in the five volume treatise on water by Franks[1, 58-61]

Water, H_2O, in the liquid state has an absorption spectrum as shown in Fig. 7.1. The data has been taken from paper III and has been measured at 37 °C. The most recent compilation of the absorption spectrum of water at 25 °C is given by Bertie and Lan.[62] The strongest absorption bands are the OH stretch band $\bar{\nu}_{1,3}$ found betweeen 3800 and 3000 cm^{-1} and the OH bend band, $\bar{\nu}_2$, at 1644 cm^{-1}. At 800 to 500 cm^{-1} one finds a broad strong absorption band caused by collective motion of water molecules, the so-called libration band $\bar{\nu}_L$. These three bands are not resolved in Fig. 7.1. A combination band $\bar{\nu}_2 + \bar{\nu}_L$ is found at 2100 cm^{-1} and a combination band $\bar{\nu}_{1,3} + \bar{\nu}_2$ is found at 5160 cm^{-1}. Overtone bands are found at approximately 6900 cm^{-1}. The major absorption bands are listed in Table 7.1.

Wavenumber / cm^{-1}	Vibration mode
500-800	Libration, broad
1644	H-O-H bend
2128	H-O-H bend + libration
3250	Fermi enhanced overtone of H-O-H bend
3450	O-H symmetric stretch
3600	O-H asymmetric stretch
5160	H-O-H bend + (a)symmetric O-H stretch
7050	O-H stretch overtone and combination

Table 7.1: Absorption bands of water as listed by Venyaminov and Prendergast.[63]

Signals from trace components are superposed on this absorption spectrum, and an absorption spectrum of an aqueous solution containing any trace component in a clinically relevant concentration will be indistinguishable by eye from the absorption spectrum of water shown in Fig. 7.1. Information about the structure of liquid water may be extracted from the water absorption spectrum and from it's dependency on temperature. For this purpose, interest focuses on the main

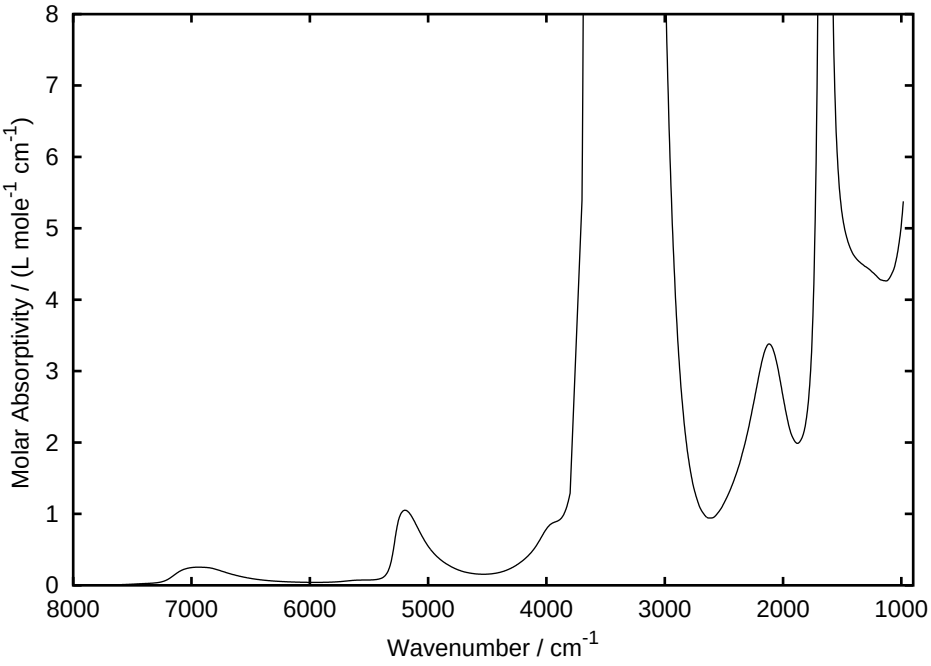

Figure 7.1: Molar absorptivity of water at 37 °C. Data has been taken from paper III.

absorption bands of water.[1, 62, 64, 65] The addition of salts,[66] acids and alkalies[67] are also known to influence the absorption properties of water. For the purpose of quantifying trace components in aqueous solutions, interest focuses on spectral regions where the influence from the water absorption is minimal and reasonable pathlengths may be employed. Paper III contributes with accurate tabulated data of the temperature variation of the absorption spectrum of water in the mid and near infrared spectral regions. The paper further contains a discussion of the influence of these variations on practical measurements of trace components in the mid and near infrared spectral regions while Paper II contributes to an improved understanding of the influence of the water absorption spectrum when spectrometers are configured for trace component detection.

8. Trace component quantification in aqueous solutions

This chapter provides a brief description of the published results, regarding the quantification of trace components in aqueous solutions, that have influenced the work presented in this thesis. These works have been focused on clinical applications. This could be regarded as a much to narrow focus, but most of the clinical applications require measurements of very low concentrations of molecules in very complex liquids. Moreover, the methods claimed to be successful are required to pass strict tests if anyone are to invest in their development into a commercial product as the consequences of instrument failure may have severe consequences. The most studied biological aqueous solutions of clinical interest are blood, blood serum. urine, and recently, spent dialysate. In addition amniotic fluid, and oral mucosa have been studied.[8, 68] A comprehensive review of the near and mid infrared applications of near and mid infrared spectroscopy with a large section devoted to measurements on biological fluids is given by Heise.[69] Vonach and Kellner have analyzed whole blood for glucose in the mid infrared region employing a transmission cell. They achieved standard errors of prediction of 13. 1 mg/dl.[13] Heise and co-workers have slightly lower standard errors of predicion for glucose, 9. 8 mg/dl using an ATR micro-Circle cell.[70] Similar results are obtained with the same technique by Haaland and co-workers.[9] Heise and co-workers have also measured protein, cholesterol and urea in whole blood.[69] The concentrations of urea, creatinine, sulphate, and phosphate has been determined in urine by the same authors.[70] standard error of prediction for urea was 13 mM. A slightly higher standard error of prediction has been obtained by Shaw, Kotowich, and Mantsch by near-infrared transmission spectroscopy, who also determined creatinine and protein.[71]

Arnold, Small and co-workers have concentrated their efforts in the combination band region, $4000 - 5000\,\mathrm{cm}^{-1}$. They have demonstrated this spectral region to be well suited for the determination of glucose, urea and other components in different fluids including blood serum and dialysate.[72, 73] In studying the blood serum, the standard error of prediction for glucose was 23 mg/dl. These author have carried out extensive investigations based on model systems with synthetically prepared samples to develop calibrations that are insensitive to temperature variations,[12] or are based on single-beam spectra.[52] The same authors have investigated the possible use of the $6500 - 5500\,\mathrm{cm}^{-1}$ spectral region, containing overtone bands, for the determination of glucose, urea and other components.[73, 74] The primary motivation for investigating the overtone band region is found in the weak absorption of water that allows deeper penetration of light. This is important in non-invasive measurements for biological purposes. The main example is the, yet to come, non-invasive glucose sensor for diabetic patients. Unfortunately, the broad and weak nature of the overtone bands found in this spectral region

makes it much less suited than the combination band region.

Commercial systems exist for measurement of trace components in milk and wine using mid infrared transmission spectroscopy.[75] The high concentrations of glucose, fructose and lactose in sugar cane juice and fruit juices may be determined with both mid and near infrared transmission spectroscopy.[76, 77]

Three of the papers contained in this thesis contributes to this field. Paper I demonstrates measurements of urea and glucose in aqueous solutions in this combination band $5000 - 4000\,\mathrm{cm}^{-1}$ spectral region with a dual-beam instrument. Paper IV presents measurements with a similar dual-beam instrument in the same spectral region for the determination of urea in spent dialysate. Paper V presents measurements of urea, glucose and phosphate in spent dialysate by mid infrared transmission spectroscopy in the $100 - 1500\,\mathrm{cm}^{-1}$ spectral region.

9. Haemodialysis treatment

This chapter gives a brief description of the causes, the consequenses and the treatment of chronical renal failure. The correct treatment is currently difficult to determine and the monitoring of trace components by FT-IR spectroscopy is a possible diagnostic tool for that purpose. The present description has been based mainly on the book edited by Eidemark and Bro.[78]

There are about 4000 patients with chronical insufficent renal function in Denmark, which has a population of approximately 6 million. Of these, approximately 1600 are subject to haemodialysis treatment. A simple scaling of these figures to a global population of 6×10^9 yields that approximately 4 million people suffers from chronical renal failure. This estimate is probably to high. Renal failure is mainly a result of a number of diseases that are more prevalent in older patients. It may be more accurate to state, that 0.07% of the population of the western world suffers from chronical renal failure. In Denmark, 20% of the patients with renal failure have diabetes. Vascular diseases are responsible for 11% of the cases. Another 26% of the cases are caused by Pyelonephritis and Glomerulonephritis, which are inflammatory disesases. Renal failure results in an accumulation of end stage products of the metabolic processes taking place in the body. Metabolic acidosis, overhydration hyperphospataemiea, hyperkalaemia and hypertension arise. Arterial hypertension is also a common cause of renal failure. The symptoms of renal failure are few. The most common symptom is fatigue. In more severe cases, anaemia, loss of appetite, dry skin, and paresthesia occur. Nearly all organs are influenced by an uremic condition, including the immune defence system, such that a patient with renal failure has less resistance against infections. With no treatment, complete renal failure is lethal.

Patients with renal failure are subject to haemodialysis treatment. In this treatment, the removal of toxins from the blood are carried out by an artificial kidney. Blood from the patient is pumped out of the patient, through a filter, where a porous membrane separates it from a stream of dialysate, and again into the patient. The difference in osmotic pressure across the porous membrane results in a diffusion of toxic components from the blood to the dialysate. A pressure gradient across the membrane is used to remove exess liquid from the patient to maintain his dry weight. In this way, the function of the kidneys are mimicked by the dialysis station. The pore size of the porous membrane determines the size of the molecules that may be removed. Numerous small and medium size molecules are removed by this process. Which of these that are toxic is under much debate. The rate of removal depends on the size of the molecule, the filter pore size, and a number of physiological factors. Some molecules are mainly extracellular and some are intracellular. Their removal is then also determined by their transport properties from and to the cells.

The efficiency of the dialysis depends on a number of parameters, such as filter type, blood flow, pressure gradient, and quality of the vascular access. A number of these parameters is individually determined for each patient. The treatment duration is long and has to be undertaken regularly. Patients are typically treated three to four hours three days a week. The correct dialysis dose is critical for the patient and monitoring the dialysis dose is therefore important. Underdialyzing a patient has severe health consequences. The current estimate of dialysis dose is based on the removal of urea. It is uncertain whether urea is toxic in itself, but it has been shown, that serum urea concentration correlates with symptoms and signs of renal failure. Urea also provides information about the patients nitrogen balance. It is the end-product of the protein breakdown process, and is directly related to the protein catabolic rate.[79] The dialysis dose is estimated from the dimensionless expression Kt/V where K is the dialyzer urea clearance, t is the treatment time and V is the urea distribution volume of the patient. This figure is required to be above 1.2 when three weekly treatments are carried out. The Kt/V value is usually estimated by the Daugirdas formula

$$Kt/V = -\ln(R - 0.008t) + (4 - 3.5R)U/W, \tag{9.1}$$

where t is the treament time in hours, R is the ratio of urea concentration in blood samples taken pre- and post- treatment, U is the ultrafiltration in L, and W is the patients weight in kg after treatment. A rough estimate is given by the formula

$$Kt/V = 0.093Kt/W, \tag{9.2}$$

where K is the in-vitro clearance of the filter, at a given blood flow, in ml/min. These estimates are neccesarily based on assumptions of a haemodialysis treatment that are following a well defined pattern. Even in patients that are in stable condition, these estimates may vary with 10-20%. Moreover, the estimate from the Daugirdas formula is made post-treatment and adjustment of treatment is usually not carried out on the basis of a single estimate of Kt/V. Since blood samples are taken monthly, this means that it may be two months before a needed adjustment is carried out. Another estimate of dialysate dose is the urea reduction ratio (URR),

$$\text{URR} = (1 - R), \tag{9.3}$$

where R is the ratio of urea concentrations in blood samples taken pre- and post-treatment as above. This ratio should be above 65% with three weekly treatments.

The continuous measurement of urea removal during haemodialysis treatment will be a useful diagnostic tool which may be used to control and optimize the treatment. In paper V, dual-beam FT-IR spectroscopy is used to carry out such an on-line monitoring. Other efforts to monitor urea concentrations in spent dialysate by optical methods include the works by Arnold, Eddy, Flannigan and

Olesberger,[73, 80] who also work with FT-IR spectroscopy in the spectral region $5000 - 4000\,\mathrm{cm}^{-1}$. A Ph.D dissertation[81] presents a method based on differential measurements at wavelengths 1485, and 1393 nm. Non-optical methods for the on-line monitoring of urea concentrations in spent dialysate exists. They are based on urease chemistry, or conductivity measurements caused by changes in ionic concentration in the dialysate. They are therefore either requiring reagents, or monitoring a secondary effect assumed to correlate with the urea concentration. An optical method would possess strong advantages over these methods in speed and accuracy. As mentioned, urea is only a secondary indicator of toxicity as it is not itself toxic. High concentrations of phosphate are known to be toxic, however. Hyperphosphateamia is linked to hyperparathyroidism, calcification, hypertension, and left ventricular hypertrophy.[82] A call for continuous monitoring of phosphate removal has recently been made.[82] Paper IV demonstrates, that phosphate may be measured with mid infrared spectroscopy together with urea and glucose. It is therefore possible to monitor these three components on-line with mid infrared transmission spectroscopy.

Acknowledgements

The supervision received from Senior Research Scientists Jimmy Bak and Peter E. Andersen of Risø National Laboratory, and Professor Stefan Andersson-Engels of Lund Institute of Technology is gratefully acknowledged.

The help and encouragement from the colleagues at the Optics and Fluid Dynamics Department, Risø National Laboratory, is gratefully acknowledged. The always friendly and helpsome colleagues at Lund Institute of Technology deserves special thanks for assistance with many adminstrative details and for the nice atmosphere that has prevailed during my particiption in courses. Senior Research Scientist Sønnik Clausen of Risø National Laboratory deserves special thanks for having the foresight to purchase an FT-IR spectrometer with two input ports when one would suffice for his purposes. Dr. Lars Thrane and Dr. Andreas Tycho are to blame for repeated intrusions and continuous demands for coffee. As head of scientific programme, Dr. Steen Hanson is to blame for luring me into this project. I beg his forgiveness for my untimely use of binoculars.

Financial support from the Danish Research Academy is gratefully acknowledged.

Summary of papers

Paper I presents measurements with a dual-beam, optical null, FT-IR instrument, also capable of measuring traditional single-beam spectra, for the quantification of urea and glucose in the near infrared spectral region $5000 - 4000\,cm^{-1}$. The results are compared with traditional single-beam measurements. The comparison shows that the dual-beam technique eliminates instrument variations and is capable of providing data that may be modeled with fewer factors yielding lower errors of prediction and better stability.

Paper II presents an analysis of noise levels in measurements of spectra of pure water and aqueous solutions at different transmission cell pathlengths. An analytical model that predicts the optimal pathlength for near infrared transmission measurements of aqueous solutions explains the results. The paper emphasizes that transmission cell pathlength should be chosen from the absorption properties of the solvent, and that it is favorable to increase pathlength when the detector would otherwise saturate. Apparent discrepancies found in the literature are explained by these results.

Paper III presents accurate measurements of the temperature variation of the absorption spectrum of water in the mid and near infrared regions. The measured molar absorptivities of water are compared to existing values found in the literature and tabulated. The temperatures are restricted to the physiologically relevant range from 30 to 42 °C. The fundamental stretching and bending bands of water are excluded. The effect of temperature on aqueous glucose solutions in the two spectral regions is also measured. The practical consequences of temperature variations and matrix effects in the two spectral regions, when trace components must be quantified, are discussed.

Paper IV presents on-line measurements of urea concentration in dialysate during treatment with the dual-beam, optical null, instrumentation presented in paper I. A simple calibration model based on synthetically prepared dialysate samples is used to predict the urea concentrations. The dual-beam instrument is demonstrated to provide accurate mesurements over a period of one month.

Paper V presents measurements of spent dialysate in the mid infrared spectral region for the simultaneous quantification of urea, glucose, and phosphate. The accuracy of the predicted concentrations are found to be comparable with that of the reference method for each of the three components.

Contributions to the papers by the author:

All work were carried out by the author with the following exceptions: Glucose measurements in paper I were carried out by first year students from Roskilde University as acknowledged in that paper. In paper IV and V, clinical chemical analysis of dialysate samples were carried out by the Clinical Chemistry

Department at the Copenhagen University Hospital. In paper V part of the measurements were carried out by T. Begovic of Risø National Laboratory. S. D. Ladefoged of the Nephrological Department, Copenhagen University Hospital bore the responsibility for the care and treatment of the patients involved in papers IV and V and contributed to the discussions of the clinical implications of analysis of dialysate. The manuscripts were written by the author with assistance from the co-authors. The author has been corresponding author of all the papers; any fault contained therein is on his head.

REFERENCES

1. Felix Franks (ed.), *The Physics and Physical Chemistry of Water,* Water a comprehensive treatise, 1, Plenum Press, New York (1972).
2. Linus Pauling, *General Chemistry,* Dover Publications Inc., New York (1970).
3. *Handbook of Near-Infrared Analysis,* Marcel Dekker, Inc., New York (2001).
4. *Infrared and Raman Spectroscopy of Biological Materials*, Marcel Dekker, Inc., New York (2000).
5. H. Zeller, P. Novak, and P. Landgraf, "Blood glucose measurement by infrared spectroscopy," *Int. J. Artif. Organs,* 12, 2, pp. 129-135 (February 1989).
6. Prashant Bhandare, Yitzhak Mendelson, Robert A. Peura, Günther Janantsch, Jürgen D. Kruse-Jarres, Ralf Marbach, and Michael H. Heise, "Multivariate Determination of Glucose in Whole Blood Using Partial Least-Squares and Artificial Neural Networks Based on Mid-Infrared Spectroscopy," *Appl. Spectrosc.,* 47, 8, pp. 1214-1221 (1993).
7. H. M. Heise and A. Bittner, "Investigation of Experimental Errors in the Quantitative Analysis of Glucose in Human Blood Plasma by ATR-IR Spectroscopy," *J. Mol. Struct.,* 348, pp. 21-24 (1995).
8. H. M. Heise and R. Marbach, "Human Oral Mucosa Studies with Varying Blood Glucose Concentration by Non-Invasive ATR-FT-IR Spectroscopy," *Cellular and Molecular. Biol.,* 44, 6, pp. 899-912 (1999).
9. Kenneth J. Ward, David M. Haaland, M. Ries Robinson, and R. Philip Eaton, "Post-Prandial Blood Glucose Determination by Quantitative Mid-Infrared Spectroscopy," *Appl. Spectrosc.,* 46, 6, pp. 959-965 (1992).
10. Jason J. Burmeister and Mark A. Arnold, "Evaluation of Measurement Sites for Noninvasive Blood Glucose Sensing with Near-Infrared Transmission Spectroscopy," *Clin. Chem.,* 45, 9, pp. 1621-1627 (1999).
11. Hoeil Chung, Mark A. Arnold, Martin Rhiel, and David W. Murhammer, "Simultaneous Measurements of Glucose, Glutamina, Ammonia, Lactate, and Glutamate in Aqueous Solutions by Near-Infrared Spectroscopy," *Appl. Spectrosc.,* 50, 2, pp. 270-276 (1996).
12. Kevin H. Hazen, Mark A. Arnold, and Gary W. Small, "Temperature-Insensitive Near-Infrared Spectroscopic Measurement of Glucose in Aqueous Solutions," *Appl. Spectrosc.,* 48, 4, pp. 477-483 (1994).
13. R. Vonach, J. Buschmann, R. Falkowski, R. Schindler, B. Lendl, and R. Kellner, "Application of Mid-Infrared Transmission Spectrometry to the

Direct Determination of Glucose in Whole Blood," *Appl. Spectrosc.,* 52, 6, pp. 820-822 (1999).

14. Takuo Yano, Takatoshi Funatsu, Ken-ichiro Suehara, and Yasuhisa Nakano, "Measurement of the concentrations of glucose and citric acid in the aqueous solution of a blood anticoagulant using near infrared spectroscopy," *J. Near Infrared Spectrosc.,* 9, pp. 43-48 (2001).

15. Gilwon Yoon, Yoen-Joo Kim, and Sangjoon Hahn, "Determination of glucose in whole blood samples by mid-infrared spectroscopy," *Appl. Opt.,* 42, 4 (1 February 2003).

16. Shmuel Argov, Jagannathan Salman, Ramesh, Ahmad Salman, Igor Sinelnikov, Jed Goldstein, Hugo Guterman, and Shaul Mordechai, "Diagnostic potential of Fourier-transform infrared microspectroscopy and advanced computational methods in colon cancer patients," *J. Biomed. Opt.,* 7, 2, pp. 248-254 (April 2002).

17. Yun Xiang Ci, Ti Yu Gao, Jun Feng, and Zhen Quan Guo, "Fourier Transform Infrared Spectroscopic Characterization of Human Breast Tissue: Implications for Breast Cancer Diagnosis," *Appl. Spectrosc.,* 53, 3, pp. 312-315 (1999).

18. Alex Pevsner and Max Diem, "Infrared Spectroscopic Studies of Major Cellular Components. Part I: The Effect of Hydration on the Spectra of Proteins," *Appl. Spectrosc.,* 55, 6, pp. 788-793 (2001).

19. A.M.K. Nilsson, D. Heinrich, J. Olajos, and S. Andersson-Engels, "Near infrared diffuse reflection and laser-induced fluorescence spectroscopy for myocardial tissue characterisation," *Spectrochim. Acta Part A,* 53, pp. 1901-1912 (1997).

20. N. B. Colthup, L. H. Daly, and S. E. Wiberley, *Introduction to Infrared and Raman Spectroscopy,* Academic Press, San Diego, California (1990).

21. Donald L. Pavia, Gary M. Lampman, and George S. Kriz, *Introduction to Spectroscopy,* Saunders College Publishing, Orlando,Florida (1996).

22. David R. Lide, (ed.), *Handbook of Chemistry and Physics*, pp. 9-74, CRC Press, Boca Raton, Florida (1995).

23. Peter R. Griffiths and James A. de Haseth, *Fourier Transform Infrared Spectrometry,* John Wiley & Sons, New York (1986).

24. Tomas Hirschfeld, "Quantitative FT-IR A detailed look at the problems involved" in *Fourier Transform Infrared Spectroscopy Applications to Chemical Systems,* ed. John R. Ferraro and Louis J. Basile, 2, Academic Press, Orlando, Florida (1979).

25. J. E. Bertie, “Apodization and Phase Correction” in *Analytical Applications of FT-IR to Molecular and Biological Systems,* ed. J. R. Durig, NATO Advanced Study Institutes, Series C -- Mathematical and Physical Sciences, 57, D. Reidel Publishing Company, Dordrecht: Holland (1980).

26. E. Oran Brigham, *The Fast Fourier Transform and its Applications,* Prentice Hall, Englewood Cliffs,New Jersey (1988).

27. William H. Press, Saul A. Teukolsky, William T. Vetterling, and Brian P. Flannery, *Numerical Recipes in C The Art of Scientific Computing,* Cambridge University Press, Cambridge (1995).

28. M. Shane Hutson and Mark S. Braiman, “Direct Phase Correction of Differential FT-IR Spectra,” *Appl. Spectrosc.*, 52, 7, pp. 974-984 (1998).

29. H. Sakai, G. A. Vanasse, and M. L. Forman, “Spectral Recovery in Fourier Spectroscopy,” *J. Opt. Soc. America,* 58, 1, pp. 84-90 (1968).

30. D. B. Chase, “Phase Correction in FT-IR,” *Appl. Spectrosc.,* 36, 3, pp. 240-244 (1982).

31. Michael A. Kinch, “Fundamental Physics of Infrared Detector Materials,” *J. Electron. Mat.,* 29, 6, pp. 809-817 (2000).

32. N. J. Harrick,, *Internal reflection spectroscopy,* Interscience Publishers,, New York (US), (1967).

33. Jan D. Miller, Mehmet Hancer, and Roger P. Sperline, “Anomalous Dispersion Effects in the IR-ATR Spectroscopy of Water,” *Appl. Spectrosc.,* 54, 1, pp. 138-143 (2000).

34. P. Fellget, “Les Progrès Recénts en spectroscopie interférentielle,” *Bellevue, Colloq. Int. C.N.R.S.,* p. 53 (1957).

35. Hillel Bar-Lev, “A Dual-Beam Infrared Interferometer Spectrometer,” *Infrared Phys.,* 7, pp. 93-98 (1967).

36. M. J. D. Low and H. Mark, “SO_2 Detection by Dual-Beam Fourier Transform Spectroscopy,” *Water, Air, and Soil Pollution,* 1, pp. 3-6 (1971).

37. George A. Vanasse, Randall E. Murphy, and Floyd H. Cook, “Double-beaming technique in Fourier spectroscopy,” *Appl. Opt.*, 15, 2, pp. 290-291 (February 1976).

38. Orr Sheperd, William Reidy, and George A. Vanasse, “Background suppression and spectral detection using double-beam interferometry: instrumentation,” *Proc. SPIE,* 191, pp. 64-70 (1979).

39. Theodore Zehnpfennig, Saul Rappaport, and George A. Vanasse, “Background suppression and spectral detection using double-beam interferometry: measurements,” *Proc. SPIE,* 191, pp. 71-78 (1979).

40. Peter R. Griffiths, “Recent Applications of Fourier Transform Infrared Spectrometry in Chemical and Environmental Analysis,” *Appl. Spectrosc.*, 31, 6, pp. 497-505 (1977).

41. H. R. Chandrasekhar, L. Genzel, and J. Kuhl, “Double-beam Fourier Spectroscopy with interferometric background compensation,” *Opt. Commun.*, 17, 1, pp. 106-110 (April 1976).

42. L. Genzel, H. R. Chandrasekhar, and J. Kuhl, “Double-beam Fourier spectroscopy with two inputs and two outputs,” *Opt. Commun.*, 18, 3, pp. 381-386 (August 1976).

43. L. Genzel and J. Kuhl, “A New Version of a Michelson Interferometer for Fourier Transform Infrared Spectroscopy,” *Infrared Phys.*, 18, pp. 113-120 (1978).

44. Donald Kuehl and Peter R. Griffiths, “Dual-Beam Fourier Transform Infrared Spectrometer,” *Anal. Chem.*, 50, 3, pp. 418-422 (March 1978).

45. Maria M. Gomez-Taylor and Peter R. Griffiths, “On-Line Identification of Gas Chromatographic Effluents by Dual-Beam Fourier Transform Infrared Spectroscopy,” *Anal. Chem.*, 59, 3, pp. 422-425 (March 1978).

46. G. J. Kemeny and P. R. Griffiths, “Improved Sensitivity in Dual-Beam Fourier Transform Infrared Spectroscopy,” *Appl. Spectrosc.*, 34, 1, pp. 95-97 (1980).

47. C. P. Tripp and M. L. Hair, “Transmission Infrared Spectra of Adsorbed Polymers Using a Dual-Beam FT-IR Instrument,” *Appl. Spectrosc.*, 46, 1, pp. 100-106 (1992).

48. C. P. Tripp and M. L. Hair, “Quantitative Infrared Spectroscopy of Polystyrene Block Copolymer Adsorbed on Mica,” *Langmuir*, 8, pp. 241-244 (1992).

49. Donald L. Beduhn and Robert L. White, “Advantages of Dual-Beam Interferometry in Fourier Transform Infrared Spectrometry,” *Appl. Spectrosc.*, 40, 5, pp. 628-632 (1986).

50. Philip R. Bevington and D. Keith Robinson, *Data Reduction and Error Analysis for the Physical Sciences,* McGraw-Hill Book Company, New York (1992).

51. Peter R. Griffiths and Bryan T. Bowie, “Measurement of the Sensitivity and Photometric Accuracy of FT-IR Spectrometers,” *Appl. Spectrosc.*, 54, 8, pp. 1192-1202 (2000).

52. Mark A. Arnold, Geng Lu, Xiangji Zhou, and Gary W. Small, “Multivariate Calibration Models Based on the Direct Analysis of Near-Infrared Single-Beam Spectra,” *Appl. Spectrosc.*, 51, 9, pp. 1330-1339 (1997).

53. Svante Wold, Kim Esbensen, and Paul Geladi, “Principal Component Analysis,” *Chemo. Intel. Lab. Sys.*, 2, pp. 37-52 (1987).

54. Harald Martens and Tormod Næs, *Multivariate calibration*, John Wiley & Sons, New York (1989).

55. Neil A. Butler and Michael C. Denham, “The peculiar shrinkage properties of partial least squares regression,” *J. Royal Stat. Soc. B*, 62, 3, pp. 585-593 (2000).

56. Eric Bouveresse and Bruce Campbell, “Transfer of Multivariate Calibration Models Based on Near-Infrared Spectrscopy” in *Handbook of Near-Infrared Analysis*, ed. Donald A. Burns and Emil W. Ciurczak, pp. 241-260, Marcel Dekker, Inc., New York (2001).

57. T. Hirschfeld, “Dynamic Range Improvement in Fourier Transform Infrared Spectrometry,” *Anal. Chem.*, 50, 8, p. 1225,1226 (July 1978).

58. Felix Franks (ed.), *Water in Crystalline Hydrates Aqueous Solutions of Simple Nonelectrolytes*, Water a comprehensive treatise, 2, Plenum Press, New York (1973).

59. Felix Franks (ed.), *Aqueous Solutions of Simple Electrolytes*, Water a comprehensive treatise, 3, Plenum Press, New York (1973).

60. Felix Franks (ed.), *Aqueous Solutions of Amphiphiles and Macromolecules*, Water a comprehensive treatise, 4, Plenum Press, New York (1975).

61. Felix Franks (ed.), *Water in Disperse Systems*, Water a comprehensive treatise, 5, Plenum Press, New York (1975).

62. John E. Bertie and Zhida Lan, “Infrared Intensities of Liquids XX: The Intensity of the OH Stretching Band of Liquid Water Revisited, and the Best Current Values of the Optical Constants of $H_2O(l)$ at 25 °C between 15000 and 1 cm^{-1},” *Appl. Spectrosc.*, 50, 8, pp. 1047-1057 (1996).

63. Sergei Venyaminov and Franklyn G. Prendergast, “Water H_2O and D_2O Molar Absorptivity in the $1000 - 4000\ cm^{-1}$ Range and Quantitative Infrared Spectroscopy of Aqueous Solutions,” *Anal. Biochem.*, 248, pp. 234-245 (1997).

64. F. O. Libnau, J. Toft, A. A. Christy, and O. M. Kvalheim, “Structure of Liquid Water Determined from Infrared Temperature Profiling and Evolutionary Curve Resolution,” *J. Am. Chem. Soc.*, 116, pp. 8311-8316 (1994).

65. Fred O. Libnau, Olav M. Kvalheim, Alfred A. Christy, and Jostein Toft, “Spectra of water in the near- and mid-infrared region,” *Vib. Spectrosc.*, 7, pp. 243-254 (1994).

66. J. J. Max, M. Trudel, and C. Chapados, “Subtraction of the water spectra from the infrared spectrum of saline solutions,” *Appl. Spectrosc.*, 52, 2, pp.

234-239 (1998).

67. J. J. Max and C. Chapados, “Subtraction of the water spectra from infrared spectra of acidic and alkaline solutions,” *Appl. Spectrosc.,* 52,, 7, pp. 963-969 (1998).

68. Kan-Zhi Liu and Henry H. Mantsch, “Simultaneous quantification from infrared spectra of glucose concentrations, lactate concentrations and lecithin/sphingomyelin ratios in amniotic fluid,” *Amer. J. Obst. Gyn..,* 180, 3, pp. 696-702 (March 1999).

69. Michael M. Heise, “Clinical Applications of Near- and Mid-Infrared Spectroscopy” in *Infrared and Raman Spectroscopy of Biological Materials,* ed. Hans-Ulrich Gremlich and Bing Yan, pp. 259-322, Marcel Dekker,Inc., New York (2000).

70. H. M. Heise, G. Voigt, P. Lampen, L. Küpper, S. Rudloff, and G. Werner, “Multivariate Calibration for the Determination of Analytes in Urine Using Mid-Infrared Attenuated Total Reflection Spectroscopy,” *Appl. Spectrosc.,* 55, 4, pp. 434-443 (2001).

71. Anthony R. Shaw, Steven Kotowich, Henry H. Mantsch, and Michael Leroux, “Quantitation of Protein, Creatinine, and Urea in Urine by Near-Infrared Spectroscopy,” *Clin. Biochem.,* 29, 1, pp. 11-19 (February 1996).

72. Kevin H. Hazen, Mark A. Arnold, and Gary W. Small, “Measurement of glucose and other analytes in undiluted serum with near-infrared transmission spectroscopy,” *Anal. Chem. Acta,* 371, pp. 255-267 (1998).

73. Christopher V. Eddy and Mark A. Arnold, “Near-Infrared Spectroscopy for Measuring Urea in Hemodialysis Fluids,” *Clin. Chem.,* 47, 7, pp. 1279-1286 (2001).

74. Kevin H. Hazen, Mark A. Arnold, and Gary W. Small, “Measurement of Glucose in Water with First-Overtone Near-Infrared Spectra,” *Appl. Spectrosc.,* 52, 12, pp. 1597-1605 (1998).

75. Foss Electric A/S, Denmark, Milkoscan^{TM}, Winescan^{TM}.

76. Frederic Cadet, “Measurement of sugar content by multidimensional analysis and mid-infrared spectroscopy,” *Talanta,* 48, pp. 867-875 (1999).

77. F. J. Rambla, S. Garrigues, and M. de la Guardia, “PLS-NIR determination of total sugar, glucose, fructose and sucrose in aqueous solutions of fruit juices,” *Anal. Chem. Acta,* 344, pp. 41-53 (1997).

78. *Dialyse,* p. Foreningen af Danske Lægestuderendes Forlag, København (2000).

79. H. J. Kemp, A. Parnham, and C. R. Tomson, “Urea kinetic modeling: a measure of dialysis adequacy,” *Ann. Clin. Biochem.,* 38, pp. 20-27 (2001).

80. Jonathon T. Olesberger, Ben Armitage, Mark A. Arnold, and Michael J. Flanigan, “Online measurement of urea concentration in spent dialysate during hemodialysis,” *Proc. SPIE*, 4624, pp. 95-105 (2002).

81. Rebecca Kupcinskas, “A method for Optical Measurement of Urea in Effluent Hemodialysate,” Ph.D Dissertation, Worchester Polytechnic Institute (2000).

82. Jean-Pierre Gutzwiller, Daniel Schneditz, Andreas R. Huber, Christian Schindler, Felix Gutzwiller, and Carlos E. Zehnder, “Estimating phosphate removal in haemodialysis: an additional tool to quantify dialysis dose,” *Nephrol. Dial. Transplant.*, 17, pp. 1037-1044 (2002).

LUND INSTITUTE OF TECHNOLOGY
Lund University

Printed by Pittney Bowes Management Services, DK
March 2003

Lund Reports on Atomic Physics, LRAP-299
ISSN 0281-2162
LUTFD2(TFAF-1052)/1-54(2003)
ISBN 91-628-5587-5